SPECTROPHOTOMETRIC STUDY OF ANALYTICAL REACTIONS OF TRIPHENYLMETHANE DYES WITH URANYL IN THE PRESENCE OF CATIONIC SURFACTANTS

Luděk JANČÁŘ, Josef HAVEL and Lumír SOMMER

Department of Analytical Chemistry, J. E. Purkyně University, 611 37 Brno

Received June 18th, 1987
Accepted November 2nd, 1987

Dedicated to the memory of Prof. Jan Horák.

Numerical analysis of absorbance data for the analytically significant UO_2^{2+}–Chromazurol B, UO_2^{2+}–Chromazurol S, and UO_2^{2+}–Eriochromcyanine R systems in the presence of the cationic surfactant Septonex^R revealed that also in micellar medium, complex equilibria establish and several complexes are formed in dependence on pH and concentration of uranyl ions, reagent, and surfactant. Based on the results, optimum conditions are found for the spectrophotometric determination of low concentration of uranium.

Triphenylmethane dyes with a salicylic functional group are proven analytical reagents for uranium[1–9]. The reaction, however, is nonselective, a number of metal ions except alkali metal and alkaline earth ions being subject to react in acid or neutral solutions[10–15]. Of reagents in this group, Chromazurol S (C.I. 43 825, 3″-sulpho-2″,6″-dichloro-3,3′-dimethyl-4-hydroxyfuchsone-5,5′-dicarboxylic acid), Eriochromazurol B (2″,6″-dichloro-3,3′-dimethyl-4-hydroxyfuchsone-5,5′-dicarboxylic acid), and Eriochromcyanine R (C.I. 43 820, 2″-sulpho-3,3′-dimethyl-4-hydroxyfuchsone-5,5′-dicarboxylic acid) have proved to serve well in the practice. With reagents of this group, cationic and nonionic surfactants (T^+, T) exhibit a marked surfactant effect; this effect brings about analytically favourable changes in the optical properties also for systems involving the UO_2^{2+} ion, thus facilitating sensitive, though nonselective, spectrophotometric determination of uranium[15–27].

Reactions of UO_2^{2+} with Chromazurol S (refs[18–24]), Eriochromcyanine R (refs[25–27]), and Eriochromazurol B (refs[16,17]) in the presence of surfactants have been employed for the spectrophotometric determination of uranium; the reaction mechanism and reaction kinetics in various experimental conditions in the absence or presence of surfactant, however, have not been as yet elucidated unambiguously. The effect of the micellar state of the surfactant on the formation, stoichiometry and structure of the forming ternary complexes with uranyl is not clear either and the role of competitive equilibria in the complex systems involving surfactant has

been underestimated. Related to this are the enhanced dispersion of absorbance values in the presence of surfactant, distortion of the linear calibration plots for the determination of uranium, mutual inconsistency of published molar absorptivities as well as the different effect of interfering ions and masking agents.

Inasmuch as spectrophotometry in the visible spectral region is still the basic method for the determination of low concentrations of uranium, understanding the reaction mechanism and establishing optimum conditions for the determination being prerequisite for obtaining accurate and precise results, the complex reaction mechanism in the ternary systems containing a triphenylmethane dye and a cationic surfactant is examined in this work by numerical analysis of spectrophotometric data using the general minimization program SQUAD-G (refs[28-30]), and the results are compared with those obtained by graphical analysis of absorbance curves. Of cationic surfactants, Septonex^R (1-ethoxycarbonylpentadecyltrimethylammonium bromide) was employed for the study of the ternary systems as well as for the spectrophotometric determination of uranium owing to its good solubility in ethanolic -aqueous solutions, stability of its stock solutions and products in the ternary systems, and high molar absorptivity of its ternary complexes with UO_2^{2+}.

EXPERIMENTAL

Chemicals and Solutions

Standard solutions of uranium ($c = 0{\cdot}189$ mol l^{-1}) were prepared from $UO_2Cl_2.2\,H_2O$ of reagent grade purity (Lachema, Brno) and standardized gravimetrically via 8-hydroxyquinolinate. The solution contained HCl in a concentration of 0·2 mol l^{-1}. Eriochromazurol B (henceforth CAB) was obtained by multiple precipitation of alkaline solution of its disodium salt (C. Erba, Italy) on acidification to pH 2·2 with 2M-HCl and multiple rinsing of the precipitate with 0·01M--HCl. The chemical was dried in a dessicator over solid KOH and equilibrated in air to constant weight. Elemental analysis revealed that the sample contained 97·82% active component with respect to the anhydrous reagent. Chromazurol S (henceforth CAS) (dihydrate) was prepared from the trisodium salt of the reagent (Geigy, Basel, or ICN Pharmaceutical, New York) by conversion to the free acid, and freed from CAB by a combined precipitation-extraction procedure[31,32]. The chemical contained 89·02% active component with respect to the dihydrate. Eriochromcyanine R (henceforth ECR) (dihydrate) was obtained by precipitation from aqueous solution of the trisodium salt (Lachema, Brno) with HCl added up to its final concentration 2 mol l^{-1}. The precipitate was collected on an S 4 frit, rinsed with 2M-HCl and water and equilibrated in air to constant weight after drying in a dessicator over solid KOH. The active component content found by elemental analysis of the equilibrated product was 89·30% with respect to the free acid dihydrate.

The purity of the refined reagents was checked by TLC on Silufol Extra Pure plates 20 × 20 cm (Kavalier, Votice) using chloroform as eluent in the ascending mode. Prior to use, the plates were activated for 30 min at 110°C and deactivated for 4 h in air at room temperature. The chromatograms were developed in Desaga cuvettes after saturation with vapours of the 1-butanol--acetic acid-water 7 : 1 : 5 system. Stock solutions of the reagents were prepared from precisely weighed amounts of the equilibrated preparations in small volumes of concentrated ammonia.

The solution was adjusted with dilute HCl to pH 9 after dilution, and the solutions were diluted to a onstant volume with bidistilled water. The reagent concentration was 1—4 mmol l^{-1}, and solutions stored no longer than a week were used.

Septonex^R (henceforth SPX) in a purity conforming to Czechoslovak Pharmacopoeia 3 (Slovakofarma, Hlohovec) was purified by dissolution in 20—50 ml of hot ethanol, filtration through an S 4 frit and precipitation dropwise with diethyl ether. The flakes obtained were filtered out and dried in a vacuum dessicator over anhydrous $CaCl_2$. Cetylpyridinium bromide (henceforth CPB) and cetyltrimethylammonium bromide (henceforth CTMA) (Lachema, Brno) were purified likewise. The concentration of the surfactants in their ethanolic stock solutions was 20 mmol l^{-1}. Zephyramin^R (benzyldimethyltetradecylammonium chloride) (henceforth ZPA) was a chemical of Dojindo, Japan, and was recrystallized twice from water and dried. Ajatin^R (benzyldimethyldodecylammonium bromide) (henceforth AJA) supplied by Zdravotnické zásobování, Prague, was frozen out, recrystallized twice from water and dried. Hyamin 1622 (benzyldimethyl-[2-[2-[*p*-(1,1,3,3-tetramethylbutyl)-phenoxy]-ethoxy]-ethyl]ammonium chloride monohydrate) (henceforth HYA) was a commercial chemical of Schuchardt, Munich. These surfactants were stored in ethanolic solutions in concentrations of 40—60 mmol l^{-1}. Solutions of the purified cationic surfactants exhibited no Tyndall effect and were stable for a minimum of 3 weeks.

Commercial ethanol was distilled on a column in the presence of EDTA. The major fraction of the distillate contained 4·3—4·4% water and 3·9—4·3% methanol. Bidistilled water was obtained on a quartz still (Heraeus, F.R.G.) and was used for all solutions.

Solutions of HCl and NH_3 (both 5 mol l^{-1}) were prepared from commercial chemicals of reagent grade purity by isothermal distillation in a dessicator. Buffers containing pyridine in a concentration of 2 mol l^{-1} (pH 6·0 or 5·6) were obtained by dilution of 15·82 g of redistilled pyridine with water, pH adjustment with HCl under pH-metric control and dilution to 100 ml. All the remaining chemicals used were of reagent grade purity.

Apparatus and Procedure

A PHM-64 pH-meter (Radiometer, Copenhagen) fitted with a G 202 B glass electrode and a K 401 saturated calomel electrode was calibrated using NBS standard buffers over the region of pH 1·68—9·18. Spectra and absorbances were recorded on a Superscan 3 UV-VIS spectrophotometer (Varian Techtron, Australia); absorbances were measured using 10—40 mm cells. A B 641 Autobalance Universal Bridge conductometer (Wayne Kerr, Canada) with a conductivity cell and a home made stalagmometer were also employed.

Computers used were an EC 1 033 (U.S.S.R.) with a 512 kB memory and a PDP 11/34 (Digital Equipment Corporation, U.S.A.) with a use memory of 64 kB. A VT 100 video terminal, a 1612 Digigraph (Czechoslovakia) and a DT 105S puncher (Zabrze, Poland) were also used.

During pH measurement, surfactants stored for a week or longer brought about a slower establishment of the glass electrode and pH differences in unstirred solution as compared to solution stirred with a magnetic stirrer (ΔpH = 0·03). The glass electrode was cleaned periodically by rinsing with hot ethanol or dimethylformamide. Ternary and binary dye complexes adsorbed on the electrodes were decomposed with 1M-HCl and dissolved in hot ethanol. During the measurement, pH was read in 20—30 s intervals without stirring.

The pH of the acid reaction mixture (50—100 ml) was adjusted with dilute ammonia, which was added continuously to the stirred solution by means of a polypropylene syringe with a polyethylene capillar tip. After pH reading, the solution was transferred repeatedly to the spectrophotometric cell and back to the solution to be adjusted in a beaker. The ultimate volume change at the end of the absorbance measurements did not exceed 1%. For the system involving ECR, the continuous mode had to be abandoned because of a considerable time instability of the weakly acid

solutions[31,32]. The order in which the reaction components were added had no significant effect on the absorbance or the time stability of the solutions; the surfactant, however, had to be added before the reagent to avoid formation of the low-soluble reagent–surfactant ion pair whose subsequent dissolution in excess surfactant may be ill-reproducible.

Data Processing

Recording of the data measured was controlled by means of the REGREC and PUNPRI programs[30,33] for the HP 9 815A computer. The REGREC program enables recording, peeling-off and storage of an absorbance data set for up to 36 wavelengths, the PUNPRI program serves for data transfer from a magnetic tape to a punch tape and printout on the thermal printer of the HP 9 815A. Data stored in the memory of the EC 1 033 or PDP 11/34 computers, punched on cards or a tape, were processed by programs such as SQUAD-G (refs[28,30,33]), PLOT 3D (ref.[34]), LETAGROP (ref.[35]), HALTAFALL-SPEFO-GRAPH (ref.[36]) or RANKANAL (refs[37,38]). The original version of the SQUAD program[39] was generalized and extended to the SQUAD-G program set in which the new version of SQUAD (ref.[40]) was also included after modification and extension. For a system comprising up to five interacting basic components, the SQUAD-G program assembly makes it possible, based on a matrix analysis of absorbance data, to determine the number of absorbing species (RANKANAL and FA 608 (ref.[41]) programs), the dissociation constants of the reagents or the equilibrium constants, stability constants of complexes in solution and their standard deviations, and sets of molar absorptivities of complexes and their standard deviations. The concentration proportions of the complexes present at a given pH, spectra of individual complexes or reagent species that are not amenable to direct experimental measurement, distribution diagrams of all species in the solution with respect to the basic components of the system, and contributions of the coloured species to the total measured absorbance are also computed and printed out. The potential of this program also includes data reading from various media (punch tape or cards, disk and diskette store), modelling spectra with a Gaussian profile and loading them with pseudorandom errors, testing various reaction models combined with a direct calculation of the stoichiometric indices of complexes included. The input data include spectra in the form of an abosrbance matrix for up to 170 solutions and 2—50 wavelengths, pH values for pH-dependent reactions, total concentrations of components, composition of expected complexes and their stability constant estimates. The PLOT 3D program and standard procedures of the Digigraph 1612 device on the EC 1033 computer were employed for spatial drawing of the experimental absorbance curves or contributions from the individual complexes to the total absorbance, e.g., in dependence on pH. By means of this program, the drawings can be rotated at will in the three-dimensional space around combinations of all coordinate axes.

RESULTS

Critical Micellar Concentrations of Some Surfactants

Conductivity and tensiometric measurements showed that for the cationic surfactants SPX, CPB, and CTMA the critical micellar concentrations (*CMC*) are lower than 1 mmol l^{-1} and that these concentrations increase with increasing ethanol content and decrease appreciably with increasing ionic strength of the solutions (Table I). The data do not disagree with published values[23,42–44] and also confirm suppression of the micelle formation with increasing concentration of ethanol. Consistent with

this fact is the disturbing effect of ethanol on the formation of the UO_2^{2+}–TPM–surfactant micell arcomplexes and the positive effect of increasing ionic strength in the elimination of distortions on the linear calibration plots for solutions with excess reagent and low concentrations of uranium.

Reactivity in Reagent–Surfactant Binary Systems

Absorbances over the 350–750 nm range for CAB or CAS solutions with $c_L = 7-35\ \mu mol\ l^{-1}$ in the presence of cationic surfactant ($c_T \leqq 1\ mmol\ l^{-1}$) at pH 6 were constant for 3 h from the solution mixing. With ECR, the solutions were only stable for 3 h at pH 9, $c_L = 40\ \mu mol\ l^{-1}$, $c_T = 0{\cdot}5-1\ mmol\ l^{-1}$. At pH $\leqq$ 6 the absorbances at wavelengths shorter than 590 nm decreased in this time period to one-half of their initial values (ref.[32]); at $\lambda < 590$ nm, however, the system is steady or else the changes in the absorbance of reagent do not manifest themselves in the total absorbance. The time decrease in absorbance observed in this case is presumably due to the conversion of the reagent to the sulphone form[31].

In dependence on pH, CAS and ECR can exist in six differently absorbing species, viz. H_5L^+, H_4L, H_3L^-, H_2L^{2-}, HL^{3-} and L^{4-}, CAB, in five species, viz. H_4L^+, H_3L, H_2L^-, HL^{2-}, and L^{3-} (refs[32,45]); appreciable absorptivity changes and bathochromic shifts of the absorption maxima occur particularly with the symmetric species. For some species the order in which the protons are split off is not unambi-

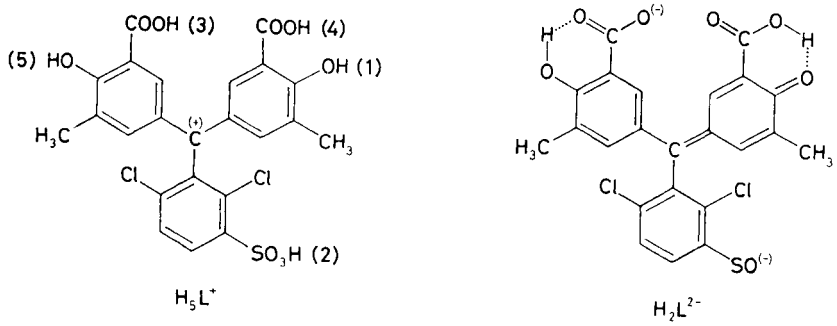

SCHEME 1

guous and this order can be different in the absence and in the presence of surfactant. The most likely sequence for CAS type reagents is indicated by numerals in Scheme 1, the probable structures for the ion pair with the tenside cation are shown in Scheme 2.

The effect of cationic surfactants on the acid-base and spectral properties of various triphenylmethane dye species has been examined spectrophotometrically recently[45–49]. In the presence of surfactant, the absorptivities of the various species change and the absorption maxima exhibit bathochromic or hypsochromic shifts. The pK_{a_i}

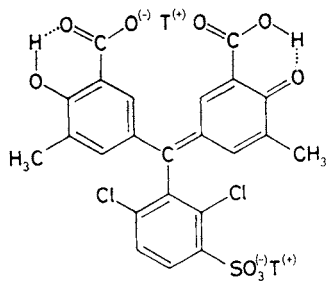

$H_2L^{2-}, 2T^+$

SCHEME 2

values experience changes as well, particularly in the region of submicellar surfactant concentrations, in comparison to solution free from surfactant, these changes being dependent on the surfactant concentration, ionic strength and presence of anions such as nitrate, perchlorate or sulphate. One to three mol of cationic surfactant bond to the anionic reagent species: $\{H_2L^-, T^+\}$, $\{HL^{2-}, 2T^+\}$ for CAB and $\{H_3L^-, T^+\}$, $\{H_2L^{2-}, 2T^+\}$ and $\{HL^{3-}, 3T^+\}$ for CAS and ECR. Association to the sulphone group leaves the optical properties unaltered. At pH < 12, no association of surfactant to the phenolic hydroxy group after the detachment of proton takes place. The formation of a stable associate with the symmetric species of the reagents, $\{H_2L^{2-}, 2T^+\}$ for CAS or ECR and $\{H_2L^-, T^+\}$ for CAB, brings about lowering in the solubility in aqueous medium and appearance of a long-wavelength absorption maximum at 582–588 nm (CAS, CAB) or 575 nm (ECR); moreover, the conditional dissociation constant $pK_a([H_3L]/[H_2L])$ decreases appreciably, and

TABLE I

Critical micellar concentrations (mmol l^{-1}) of surfactants in dependence on concentration of ethanol (conductivity measurements) and ionic strength adjusted with NaCl (tensiometric measurements)

Surfactant	φ_{EtOH}, %			I			
	0	10	20	0	0·01	0·1	0·5
SPX	0·810	0·925	1·25	0·825	0·325	0·111	0·102
CPB	0·750	0·790	0·95	0·775	0·370	0·135	0·123
CTMA	0·875	0·935	1·17	0·930	0·425	0·180	0·163

$pK_a([H_2L]/[HL])$ increases for CAS and ECR; for CAB this value also decreases with increasing c_T. The changes cease to occur after surpassing the *CMC* of surfactant and a small back effect is observed at a high excess of surfactant[50], which can be due to changes in the micelle structure[51,52]. The values of the $pK_a([H_2L]/[HL])$ conditional constant, which characterize the acid-base equilibria of the reagents and are the most important for the study of the systems involving UO_2^{2+} and surfactant, were obtained by numerical analysis of the absorbance–pH curves by the SQUAD-G program; the conditions used and results obtained are given in Table II. For CAB in the presence of Septonex^R, the pK_a value decreases for surfactant concentrations increasing up to 1 mmol l^{-1} whereas starting from a concentration of 2 mmol l^{-1} this value increases again. Analogously, the molar absorptivity at λ_{max} 510 nm (H_2L) and 430 nm (HL) increases and later decreases again. The absorption curves in dependence on surfactant concentration at pH 7·95 or 7·55 and c_L = 3·5 μmol l^{-1}, over the region of c_T = 0·875 μmol l^{-1} to 17·5 mmol l^{-1}, exhibit a shift of λ_{max} from 423 nm to 431 nm for HL^{2-} at the limiting c_T value. The isosbestic points at 560 and 525 nm correspond to the conversions of HL^{2-} to $\{HL^{2-}, 2\,T^+\}$ and $\{HL^{2-}, 2\,T^+\}$ to $\{HL^{2-}, 2\,T^+\}$ T_{mic}, respectively. The rapid drop in the absorbances

TABLE II

Values of $pK_a([H_2L]/[HL])$ for the principal dissociation equilibrium of reagents and their binary systems with Septonex^R, calculated by using the SQUAD-G program; φ_{EtOH} = 5%, I = 0·05

Reagent	c_L μmol l^{-1}	c_T mmol l^{-1}	Number of pH values	pH	$s(A)$	U	$pK_a([H_2L]/[HL])$
CAB[a]	14	0	27	3·36–8·15	0·002	0·002	4·872 ± 0·002
	35	0·3	22	2·28–8·10	0·007	0·027	4·819 ± 0·004
	70	1·0	27	2·30–8·42	0·009	0·060	4·754 ± 0·002
	35	1·0	27	2·25–7·97	0·007	0·029	4·730 ± 0·004
	24	1·0	27	2·22–7·97	0·006	0·021	4·722 ± 0·004
	14	1·0	27	2·27–8·31	0·002	0·004	4·701 ± 0·003
	7	1·0	27	2·29–8·09	0·002	0·004	4·707 ± 0·005
	24	5·0	27	2·46–8·21	0·004	0·009	4·740 ± 0·002
CAS[b]	24	0	27	3·50–8·90	0·002	0·004	4·931 ± 0·002
	24	1·0	23	2·50–8·55	0·004	0·008	4·937 ± 0·003
	7	1·0	23	2·55–8·63	0·002	0·002	4·968 ± 0·005
ECR[c]	24	0	28	3·52–9·17	0·003	0·005	5·660 ± 0·003
	24	1·0	28	3·23–8·45	0·003	0·005	5·729 ± 0·002

[a] For 28 wavelengths over the 660–400 nm range; [b] for 28 wavelengths over the 645–400 nm range; [c] for 28 wavelengths over the 640–400 nm range.

at 420 or 455 nm for solutions at pH 7·95 is a consequence of the formation of the low-soluble reagent–surfactant binary associate, which dissolves on its interaction with the surfactant micelles at $c_T < 0{\cdot}1$ mmol l^{-1}, whereupon the absorbances increase. Based on the shift of the pK_a values and the molar absorptivity data set for the H_2L^- and HL^{2-} species ($c_L = 24{\cdot}5$ μmol l^{-1}) over the Septonex^R concentration region $c_T = 0{\cdot}3-1$ mmol l^{-1} and for 54 solutions over the acidity region of pH 2·22–7·97 and the wavelength region of 660–400 nm, the $\log \beta_1 = 5{\cdot}39 \pm 0{\cdot}09$ stability constant for the $\{H_2L, T\}$ associate and $\log \beta_2 = 8{\cdot}77 \pm 0{\cdot}09$ stability constant for the $\{HL, 2T\}$ associate were calculated at $I = 0{\cdot}05$ and ethanol content of the aqueous-ethanolic solvent $\varphi_{EtOH} = 5\%$ (v/v); $\varepsilon(H_2L, T) = (2{\cdot}28 \pm 0{\cdot}04) . 10^4$ l mol^{-1} cm^{-1} (510 nm), $\varepsilon(HL, 2T) = (1{\cdot}96 \pm 0{\cdot}02) . 10^4$ l mol^{-1} cm^{-1} (430 nm).

Interactions in the UO_2^{2+}–Triphenylmethane Dye–Surfactant Ternary Systems

In the presence of cationic surfactant in a submicellar or micellar concentration, λ_{max} of the absorption curves of solutions with a low excess of reagent shifts to longer wavelengths and the molar absorptivity increases considerably in comparison to the dye–surfactant or dye–uranyl binary systems[16-27]. The absorptivity, however, is affected substantially by the solution composition, reagent concentration and surfactant kind and concentration. With HYA, ZPA, and AJA the tenside effect was highest at higher surfactant concentrations, which is related to the higher CMC (<1 mmol l^{-1}); the decomposing effect of surfactant on the ternary complexes with UO_2^{2+}, however, is less marked. In systems with CAB and surfactants such as ZPA, AJA, CTMA, CPB, the absorbance in the long-wavelength region develops for 90–180 min due to a slower interaction with the micelle. The shape of the absorption curves over the 500–700 nm region depends on the concentrations of both the reagent and surfactant and on pH. Data for systems with a low excess of reagent are given in Table III. The fact that the absorbance curves form isosbestic points gives evidence of a defined interaction with the micelle in the ternary system. The absorption spectra in dependence on the surfactant concentration indicate formation of various complex species. The long-wavelength absorption maximum at $c_T > CMC$ corresponds to the formation of the ternary ionic associate or several associates with defined stoichiometric composition, the shorter-wavelength absorption maximum at $c_T < CMC$ corresponds to the interaction of the ternary complex with the micelle, and the short-wavelength maximum at $c_T \gg CMC$ corresponds to the decomposition of the micellar complexes by the excess surfactant giving rise to uranyl–ligand and ligand–surfactant binary species. Typical spectra are shown in Fig. 1. The different optimum c_T values for attaining the highest conditional molar absorptivity in the ternary system and the different c_T values for the decomposition of the ternary micellar complex for different surfactants are due to the

differences in their *CMC*, structure and stability of their binary associates with the reagent.

UO_2^{2+}–CAB–SPX *Ternary System*

Figs 2 and 3 demonstrate that the absorption curves of solutions with excess uranium differ in shape from those of solutions with excess reagent. As the excess of the reagent is increased, the λ_{max} value at the optimum pH 5·6 shifts to shorter wavelengths and the corresponding conditional molar absorptivity decreases; this absorptivity is highest for solutions with excess uranium (Table IV). The absorption spectra in nitrate medium do not differ from those in chloride medium.

TABLE III

Effect of cationic surfactants on the optical properties of the UO_2^{2+}–CAB–surfactant and UO_2^{2+}–CAS–surfactant ternary systems at $I = 0{\cdot}05$ (HCl + NH_3)

Surfactant	c_T mmol l^{-1}	λ_{max} nm	pH_{opt}	c_T mmol l^{-1}	λ_{opt} nm	$\bar{\varepsilon}_{cond} \cdot 10^{-4}$ l mol^{-1} cm^{-1}
UO_2^{2+}–CAB–surfactant, $c_M = 7{\cdot}1$ μmol l^{-1}, $c_L = 35{\cdot}2$ μmol l^{-1}, $\varphi_{EtOH} = 5\%$ or 10% (v/v)						
SPX	<0·6	650	–	–	–	–
	0·2–4	625–630	5·6	4	630	10·530
	6–20	630, 593	–	–	–	–
CPB	0·1	653	–	–	–	–
	0·2–1	623, 650	6·0	0·2	623	10·790
	2–10	625, 597	–	–	–	–
	10	625, 597	–	–	–	–
CTMA	<0·6	662, 654	–	–	–	–
	0·2–0·8	623	6·0	0·2	623	–
	1–20	625–628, 600	–	10	627	10·550
HYA	7	650	–	–	–	–
	2	629, 605	5·5	20	593	11·270
	2–30	593, 605	–	–	–	–
ZPA	0·4	660	–	–	–	–
	<5	658	–	–	–	–
	0·6–10	623, 595	5·0	20	609	9·730
	>10	595, 609	–	–	–	–
AJA	3	626, 656	–	–	–	–
	5–10	609, 593	5·0	50	593	10·365
	10	593	–	–	–	–

TABLE III
(*Continued*)

Surfactant	c_T mmol l^{-1}	λ_{max} nm	pH_{opt}	c_T mmol l^{-1}	λ_{opt} nm	$\bar{\varepsilon}_{cond} \cdot 10^{-4}$ l mol^{-1} cm^{-1}
UO_2^{2+}-CAS-surfactant, $c_M = 5$ μmol l^{-1}, $c_L = 15$ μmol l^{-1}, $\varphi_{EtOH} = 5\%$ (v/v)						
SPX	0·01—0·1	653, 613, 588	—	—	—	—
	0·25—1·2	611—614	6·0	1	612	14·700
	2—10	595, 600	—	—	—	—
CPB	0·01—0·1	637, 612, 588	—	—	—	—
	0·2—1	613	5·75	1	613	9·100
	2·5—20	595, 616	—	—	—	—
CTMA	0·01—0·25	651, 615, 598	—	—	—	—
	0·5—2	614, 598	5·75	1·25	614	9·200
	2·5—20	575, 598, 615	—	—	—	—
HYA	0·05—0·3	646, 616, 595	—	—	—	—
	0·5—1	610, 593	—	—	—	—
	2—50	593, 650	5·75	20	593	11·900
ZPA	0·05—0·25	646, 620, 598	—	—	—	—
	0·5—2	613, 596	—	—	—	—
	5—50	613, 596	5·75	10	596	12·100
AJA	0·1—0·5	653, 620, 593	—	—	—	—
	1—2	611, 593	—	—	—	—
	5—7·5	593, 611	5·75	20	593	12·500

Absorbance–pH curves were measured at $c_M = 350-3{\cdot}5$ μmol l^{-1}, $c_L = 7$ to 70 μmol l^{-1}, $c_T = 0{\cdot}17-15$ mmol l^{-1}, $\varphi_{EtOH} = 5\%$ (v/v), $I = 0{\cdot}05$ over the region of pH 2·0—9·8 for 28 wavelengths within the 660—400 nm range. Typical curves are shown in Figs 4 and 5. For solutions with various excess of uranium, two characteristic formation ranges appear at pH 2·0—5·0 and pH 5·0—7·0. For solutions with excess reagent, there are four such ranges, viz. pH 2·0—4·0, pH 4·0—5·9, pH 5·9—8·0, and pH 8·0—9·8 and for equimolar solutions, three, viz. pH 2·0—5·5, pH 5·5—7·5, and pH 7·5—9·8. The shift of the curves to lower pH with increasing concentrations of the components (uranyl, ligand) at a constant concentration of surfactant bears out the formation and stabilization of the ternary complex. If the surfactant concentration is increased, the curves shift to higher pH values, the conditional molar absorptivity first increases and later decreases and λ_{max} shifts to shorter wavelengths. These changes are most pronounced in equimolar solutions at $c_T \geqq 10$ mmol l^{-1}. The absorbance–pH curves also shift from pH 3·8 to higher

pH with increasing concentration of reagent at a constant concentration of surfactant; they pass through an inflection point, and the absorbance in the horizontal branch drops rapidly. The changes in the pH curves are a consequence of a more hindered formation of the ternary complex with the surfactant at pH > 4, its interaction with the micelle and, ultimately, competitive equilibria resulting in a gradual decomposition of the ternary complex and formation of stable surfactant–reagent binary associates. In nitrate solutions at $I = 0{\cdot}05$, the absorbance–pH curves for solutions

TABLE IV

Optical characteristics of the UO_2^{2+}–CAB–SPX system; $I = 0{\cdot}05$ (HCl + NH_3)

c_M μmol l^{-1}	c_L μmol l^{-1}	c_T mmol l^{-1}	φ_{EtOH} %	pH_{opt}	λ_{max} nm	$\varepsilon \cdot 10^{-4}$ l mol^{-1} cm^{-1}
189	7	1·0	5	5·0	635	14·150
7·1	21	0·5	10	5·7	632	11·055
7·1	21	0·5	10	6·0	632	9·860[a]
7·1	35	0·5	10	5·7	626	10·100
7·0	70	0	5	5·7	612	2·555
0	35	0·5	10	2·3	512	2·290
				8·0	429	1·985

[a] $I = 0{\cdot}05$ (HNO_3 + NH_3)

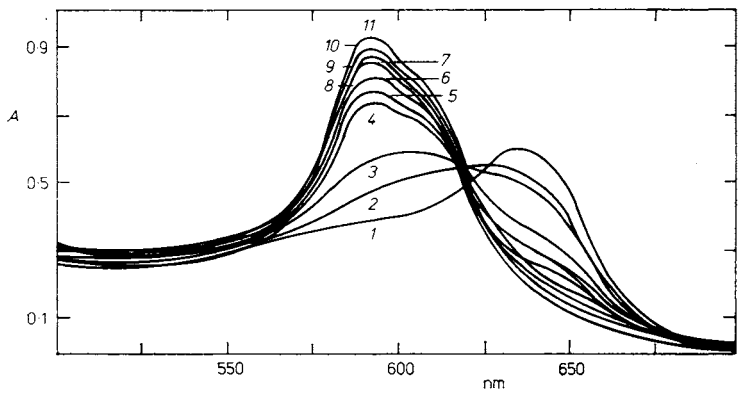

FIG. 1

Absorption of the UO_2^{2+}–CAB–HYA system; $c_M = 7$ μmol l^{-1}, $c_L = 35$ μmol l^{-1}, $\varphi_{EtOH} =$ = 10%, $I = 0{\cdot}05$, c_T (mmol l^{-1}): *1* 0·5, *2* 1, *3* 1·5, *4* 2·25, *5* 3, *6* 4·5, *7* 6, *8* 7·5, *9* 9, *10* 15, *11* 30

with excess reagent exhibit a lower absorbance and the region of existence of ternary complexes is broader. In nitrate medium the reagents exhibit higher pK_a values, and a more stable $\{NO_3^-, T^+\}$ associate with the surfactant is formed[45,50], so that the effect of the excess reagent and surfactant is weakened on the decomposition of the ternary complex.

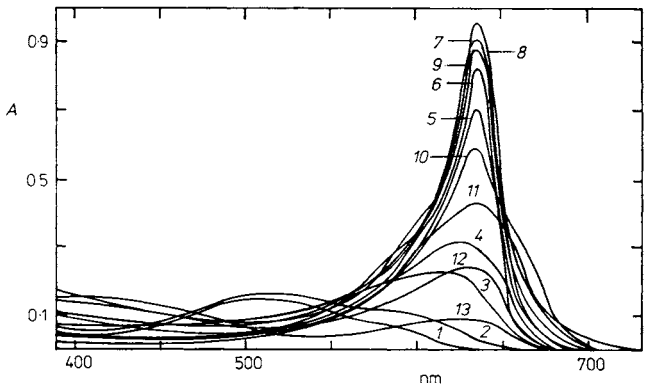

FIG. 2

Absorption spectra of the UO_2^{2+}–CAB–SPX system with excess uranium; $c_M = 190$ μmol l^{-1}, $c_L = 7$ μmol l^{-1}, $c_T = 1$ mmol $^{-1}$, $\varphi_{EtOH} = 5\%$, pH: *1* 1·51, *2* 2·37, *3* 2·91, *4* 3·18, *5* 3·45, *6* 3·71, *7* 4·32, *8* 4·62, *9* 5·60, *10* 7·05, *11* 7·73, *12* 8·60, *13* 9·33

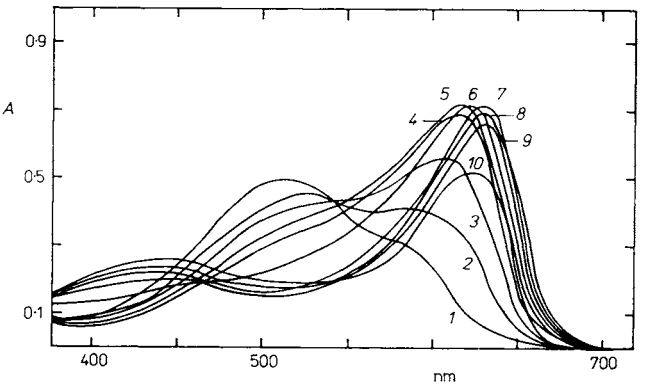

FIG. 3

Absorption spectra of the UO_2^{2+}–CAB–SPX system with excess reagent; $c_M = 7{\cdot}1$ μmol l^{-1}, $c_L = 21{\cdot}3$ μmol l^{-1}, $c_T = 0{\cdot}5$ mmol l^{-1}, $\varphi_{EtOH} = 10\%$, pH: *1* 1·92, *2* 3·17, *3* 3·52, *4* 3·95, *5* 4·37, *6* 5·25, *7* 5·82, *8* 6·26, *9* 6·56, *10* 7·23

The absorption spectra in dependence on the concentration of reagent at pH 5·6 and $c_T = 1$ mmol l^{-1} form an isosbestic point at 623 nm and the maximum found at 635 nm for $p_L = c_L/c_M = 1$ shifts to shorter wavelengths; molar absorptivity relative to c_M decreases. The ΔA vs c_L differential dependences at pH 4 and 6 have a plateau only for the isosbestic point wavelength, at higher wavelengths they attain a maximum at a ligand excess of $p_L = 1{\cdot}4$ and then drop rapidly. The set of absorption curves in dependence on c_T at the optimum pH 5·6 and $p_L = 3{\cdot}5$ forms two pairs of isosbestic points, viz. at 597 and 745 nm for $c_T = 0{\cdot}2-2$ mmol l^{-1} and at 581 and 603 nm for $c_T = 5-20$ mmol l^{-1}. At the same time, the absorption maximum undergoes a bathochromic shift to 633 nm and later it returns to shorter

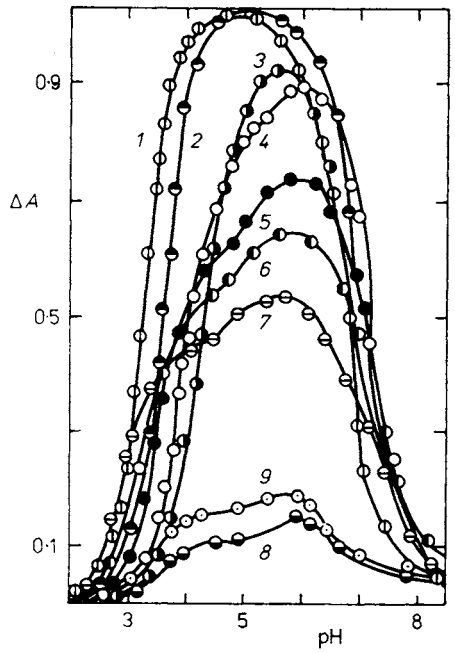

FIG. 4

Absorbance–pH curves of the UO_2^{2+}–CAB–SPX system at 635 nm; $c_M = 7-350$ μmol . l^{-1}, $c_L = 7-70$ μmol l^{-1}, $c_T = 1$ mmol . l^{-1}, $p_L = c_L/c_M$: *1* 0·02, *2* 0·1, *3* 1·0, fi 2·0, *5* 3·5, *6* 5·0, *7* 10·0; UO_2^{2+}–CAB binary system, $\varphi_{EtOH} = 5\%$, $I = 0{\cdot}05$ (HCl + NH_3): *8* 10·0, *9* 10·0, 615 nm

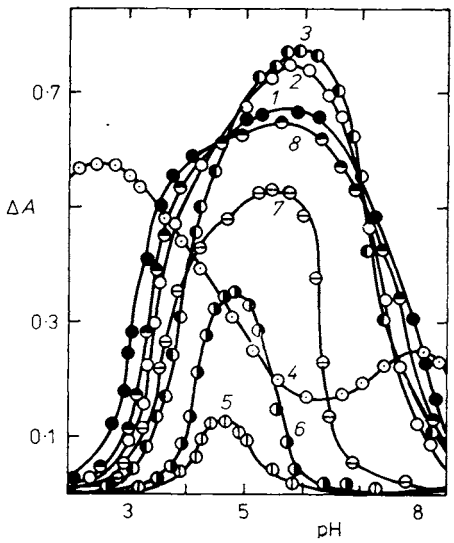

FIG. 5

Absorbance–pH curves of the UO_2^{2+}–CAB–SPX system with excess reagent at 635 nm; $c_M = 7$ μmol l^{-1}, $c_L = 24{\cdot}5$ μmol l^{-1}, $c_T = 0{\cdot}3-5$ mmol l^{-1}, $I = 0{\cdot}05$ (HCl + NH_3), $\varphi_{EtOH} = 5\%$; $p_{T(L)} = c_T/c_L$: *1* 12, *2* 41, *3* 204, *4* 12 (520 nm), *5* 2 150 ($p_L = c_L/c_M = 1{\cdot}0$, $c_T = 15$ mmol l^{-1}), *6* 1 071 ($p_L = 2{\cdot}0$, $c_T = 15$ mmol l^{-1}), *7* 214 ($p_L = 10$, $c_T = 15$ mmol l^{-1}), *8* 41 ($I = 0{\cdot}05$ (HNO_3 + NH_3))

wavelengths, and the conditional absorption coefficient related to the concentration of uranium increases and at $c_T < 2$ mmol l^{-1} decreases. The $\Delta A = f(c_T)$ difference curves for the wavelength region of 603–645 nm and at pH 5·6 increase first with increasing surfactant concentration to attain the maximum at $c_T = 0{\cdot}85$ mmol l^{-1} for $p_L = 1{\cdot}6$ and at $c_T = 3{\cdot}3$ mmol l^{-1} for $p_L = 5{\cdot}0$, later they decrease and are time unstable. For all the $\Delta A = f(c_T)$ dependences measured, the differential absorbance was highest for excess surfactant, $p_{T(L)} = c_T/c_L = 80{\cdot}9-94{\cdot}3$, hence, in the region of micellar concentration of the tenside. The above facts characterize stabilization of the uranyl–ligand–surfactant ternary complex in the micellar medium of the surfactant and competitive equilibria between the ternary and binary complexes in solutions with a high excess of surfactant (Fig. 6).

The $\Delta A = f(c_M)$ curves were studied for the following concentrations (c_L, μmol . l^{-1}, and c_T, mmol l^{-1}): *a*) 10, 0·8; *b*) 10, 1; *c*) 40, 1; *d*) 80, 1; *e*) 10, 2·5; and *f*) 20, 0·6, invariably at $\varphi_{EtOH} = 5\%$, pH 5·6 and $I = 0{\cdot}05$ (HCl + NH_3) for 28 wavelengths over the region of 660–400 nm. Examples are shown in Fig. 7. The shape of the dependences as well as the absorption curves for the corresponding conditions indicate, by the existence of isosbestic points at 500 nm for $c_M = 0{\cdot}5-3{\cdot}5$ μmol l^{-1} and 535 nm for $c_M = 5-11$ μmol l^{-1} and by the bending of the dependences at low uranium concentrations, that several defined reactions occur within the uranium concentration region treated. With increasing uranium concentration, the absorption maximum of the curves shifts from 615 nm at $p_L = 40$ to 635 nm at $p_L =$

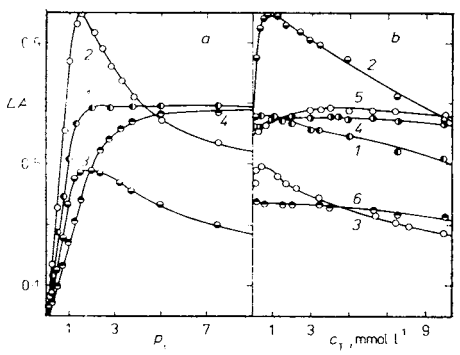

FIG. 6

$\Delta A = f(c_L)$ and $\Delta A = f(c_T)$ dependences for the UO_2^{2+}–CAB–SPX system at pH 5·6. *a* $c_M = 7$ μmol l^{-1}, $c_T = 1$ mmol l^{-1}; *b* $c_M = 7$ μmol l^{-1}, $c_L = 10$ or 35 μmol l^{-1}. Curves (λ, nm): *a* *1* 602, *2* 635, *3* 650, *4* 620 (pH 3·99); *b* *1* 620, *2* 635, *3* 650 ($c_L =$ = 10 μmol l^{-1}); *4* 620, *5* 635, *6* 650 ($c_L =$ = 35 μmol l^{-1})

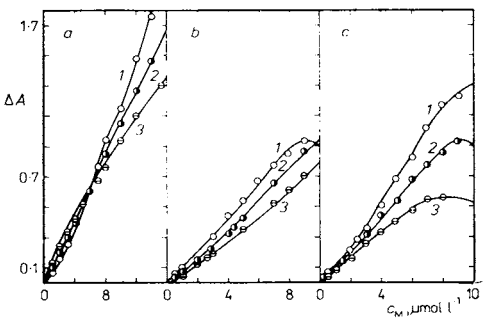

FIG. 7

$\Delta A = f(c_M)$ dependences for the UO_2^{2+}–CAB–SPX system at pH 5·6. *a* $c_L =$ = 20 μmol l^{-1}, $c_T = 0{\cdot}6$ mmol l^{-1}, λ (nm): *1* 635, *2* 625, *3* 615; *b* $c_T = 1$ mmol l^{-1}, c_T (mmol l^{-1}): λ = 635 nm c_L (μmol l^{-1}): *1* 10, *2* 40, *3* 80; *c* $c_L = 10$ μmol l^{-1}, c_T (mmol l^{-1}): λ = 635 nm, *1* 0·8, *2* 1, *3* 2·5

= 1·5. Fig. 7 and Table V demonstrate that the $\Delta A = f(c_M)$ dependence has the highest slope at $c_L = 10$ μmol l^{-1} and $c_T = 0{\cdot}8$ mmol l^{-1} but it is not linear over the $c_M = 0{\cdot}5-1{\cdot}5$ μmol l^{-1} region. At 635 nm, the slope of the linear dependences of $\Delta A = f(c_M)$ decreases with increasing c_L, at the same time, however, the curves for $\lambda < 630$ nm linearize. The slope of the $\Delta A = f(c_M)$ dependence also decreases with increasing c_T, which agrees with the shape of the $\Delta A = f(c_T)$ dependence, At $c_T > 5$ mmol l^{-1} and $c_L = 10$ μmol l^{-1} the absorbances decrease rapidly with time. At $c_L = 10-80$ μmol . l^{-1} and $c_T = 0{\cdot}6-2{\cdot}5$ mmol l^{-1} the $\Delta A = f(c_M)$ dependences are linear over the entire uranium concentration region only at 623 nm, which is the wavelength of the isosbestic point of the absorption curves n dependence on c_L. The shape of the $\Delta A = f(c_M)$ dependences is clearly affected

TABLE V

Evaluation of $A = f(c_M)$ dependences in UO_2^{2+}–CAB–SPX system; $\varphi_{EtOH} = 5\%$, $I = 0{\cdot}05$ ($HCl + NH_3$)

c_L μmol l^{-1}	c_T mmol l^{-1}	c_M μmol l^{-1}	λ nm	$\varepsilon \pm d(\varepsilon)$[a] l mol^{-1} cm^{-1}	$A_0 \pm d(A_0)$	A_0(exp)
10	0·8	0·5—9	625	109 560 ± 730	0·012 ± 0·003	0·015
			630	133 340 ± 1 660	−0·028 ± 0·008	0·012
			635	143 645 ± 1 190	−0·063 ± 0·006	0·010
10	1·0	0·5—7	625	88 600 ± 2 170	0·033 ± 0·009	0·014
			630	105 790 ± 1 790	0·006 ± 0·007	0·012
			635	115 000 ± 2 080	−0·015 ± 0·008	0·009
40	1·0	0·5—9	625	98 780 ± 1 460	0·002 ± 0·007	0·023
			630	102 100 ± 2 460	−0·033 ± 0·012	0·018
			635	100 110 ± 3 330	−0·058 ± 0·017	0·014
80	1·0	0·5—10	625	88 060 ± 810	0·032 ± 0·005	0·059
			630	85 140 ± 860	−0·003 ± 0·005	0·046
			635	79 590 ± 1 190	−0·035 ± 0·007	0·034
10	2·5	0·5—7	625	64 980 ± 4 170	0·043 ± 0·016	0·011
			630	75 860 ± 3 600	0·022 ± 0·014	0·009
			635	76 500 ± 3 200	0·017 ± 0·014	0·008
20	0·6	0·5—7	625	104 120 ± 1 140	0·003 ± 0·006	0·019
			630	115 540 ± 2 230	−0·038 ± 0·013	0·015
			635	121 890 ± 3 010	−0·085 ± 0·018	0·012

[a] $d(\varepsilon)$, $d(A_0)$ are parameter errors calculated by linear regression of data set for different c_M, A_0, and A_0(exp) are the calculated and experimental intercepts, respectively.

by the interaction of the reagent in excess surfactant or surfactant in excess reagent, and also by the formation of another ternary complex in solution with excess reagent.

UO_2^{2+}–CAS–SPX *Ternary System*

The data published previously[24] were supplemented with a detailed study of absorbance dependences for numerical data analysis. The absorption spectra of solutions with a concentration excess of uranium ($p_M = c_M/c_L = 27$) and solutions with a small excess of reagent ($p_L = 3$) in dependence on pH exhibit absorbance changes in the characteristic double maximum range at 595 and 612 nm (see also refs[20,24]). The marked absorbance decrease in the 595–612 nm range at pH > 6 in the presence of excess reagent is associated with the decomposition of the UO_2^{2+}–CAS–SPX ternary complex in favour of surfactant–reagent binary associates (Figs 8, 9). The spectral characteristics of the system under various conditions are summarized in Table VI. The absorbance–pH curves were interpreted for wide concentration regions, viz. $c_M = 7{\cdot}1-350\ \mu mol\ l^{-1}$, $c_L = 7-24{\cdot}6\ \mu mol\ l^{-1}$ ($p_L = 0{\cdot}02-3{\cdot}5$), at $c_T = 1\ mmol\ l^{-1}$ ($p_{T(L)} = 41-143$) over the region of pH 2·0–8·7 for 28 wavelengths within the 564–400 nm region (Fig. 10). The mutual positions and shifts of the curves are similar as with the UO_2^{2+}–CAB–SPX system. The pH curves of solutions with excess uranium display two characteristic regions, viz. pH 2·0–5·5 and pH 5·5–7·5, the absorbance–pH curves for equimolar solutions also exhibit two regions, viz. pH 2·0–6·0 and pH 6·0–9·0. A significant absorbance drop is observed at pH ≧ 6·3. In comparison to curves for equimolar solutions, those for solutions with excess reagent at the same c_T are shifted to a more acidic region and exhibit four characteristic pH regions. viz. pH 2·0–4·0, pH 4·0–6·1, pH 6·1–7·3, and pH 7·3–9·0. In this case, also the curves for solutions with excess cation and reagent shift to lower pH with increasing concentration of reagent or metal, and in the presence of a high excess of surfactant, the absorbance curves shift to higher pH and the conditional molar absorptivities with respect to uranium decrease.

Absorption spectra of solutions in dependence on c_L over the region of 4·2 to 70 $\mu mol\ l^{-1}$ at $c_T = 1\ mmol\ l^{-1}$ and pH 6·0 indicate a defined equilibrium. The curves form isosbestic points at 590 and 629 nm, λ_{max} shifts with increasing concentration of reagent from 613 nm ($p_L = 1{\cdot}5$) to 611 nm ($p_L = 10$), and at $p_L > 2{\cdot}5$ the conditional molar absorptivity for uranium at 612 nm decreases appreciably. The differential curves $\Delta A = f(c_L)$ at pH 6 attain the maximum absorbance for λ_{max} 612 nm at $p_L = 3{\cdot}57$ and the absorbance decreases markedly at higher concentrations of reagent; only at 500–590 nm the dependence at higher concentrations of reagent forms a plateau. The absorption spectra in dependence on c_T at $c_L = 21\ \mu mol\ .\ l^{-1}$ and the optimum pH 6 exhibit a pair of isosbestic points at 590 and 638 nm

for $c_T \leqq$ CMC and at 517 and 597 nm for $c_T = 3-8$ mmol l^{-1}. In this case the absorbance, and hence the molar absorptivity, at 612 nm decreases with increasing concentration of reagent while the absorbance at 595 nm increases (see also ref.[24]). The $\Delta A = f(c_T)$ difference dependences for 597–638 nm wavelengths increase to attain a maximum at $c_T = 1{\cdot}25$ mmol l^{-1}, and finally a decrease follows. As com-

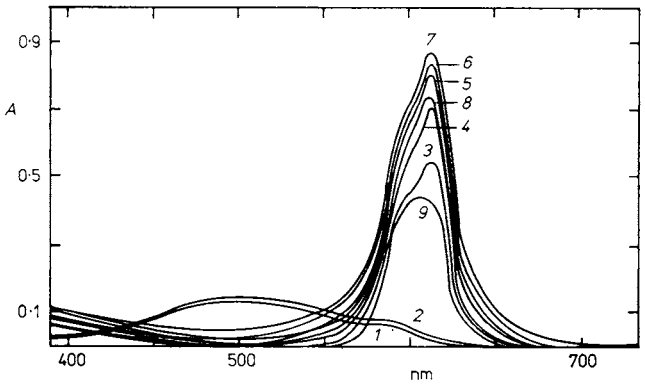

FIG. 8

Absorption spectra of the UO_2^{2+}–CAS–SPX system with excess uranium; $c_M = 190$ μmol l^{-1}, $c_L = 7$ μmol l^{-1}, $c_T = 1$ mmol l^{-1}, $\varphi_{EtOH} = 5\%$, pH: *1* 1·41, *2* 2·39, *3* 3·30, *4* 3·50, *5* 3·80, *6* 4·17, *7* 4·71, *8* 5·60, *9* 8·17

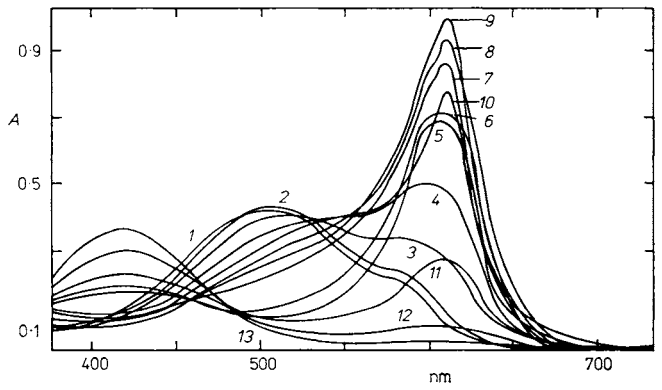

FIG. 9

Absorption spectra of the UO_2^{2+}–CAS–SPX system with excess reagent; $c_M = 7{\cdot}1$ μmol l^{-1}, $c_L = 21{\cdot}3$ μmol l^{-1}, $c_T = 0{\cdot}5$ mmol l^{-1}, $\varphi_{EtOH} = 10\%$, pH: *1* 1·91, *2* 2·73, *3* 3·21, *4* 3·56, *5* 3·87, *6* 4·22, *7* 4·88, *8* 5·63, *9* 5·95, *10* 6·55, *11* 6·92, *12* 7·28, *13* 8·55

pared to chloride medium, in nitrate medium the formation of the ternary complex occurs at higher pH and the molar absorptivity for uranium is lower, viz. $\varepsilon = 11{\cdot}40 \,.\, 10^4$ l mol^{-1} cm^{-1} as against the $13{\cdot}90 \,.\, 10^4$ l mol^{-1} cm^{-1} for the chloride medium. This can account for the disagreement with the molar absorptivities published

TABLE VI

Optical characteristics of the UO_2^{2+}–CAS–SPX system; $\varphi_{EtOH} = 5\%$ or 10%, $I = 0{\cdot}05$ (HCl + NH_3)

c_M μmol l^{-1}	c_L μmol l^{-1}	c_T mmol l^{-1}	pH_{opt}	λ_{max}	$\varepsilon_{cond} \,.\, 10^{-4}$ l mol^{-1} cm^{-1}
189	7·0	1·0	4·7	612; 595	11·87; 8·72
7·1	21	0·5	6·0	612; 595	13·76; 11·15
7·1	35	0·5	6·0	612; 595	12·50; 10·79
350	7·0	0	4·7[a]	592	4·85
7·0	49	0	5·0[a]	575	1·73
0	35	0·5	2·9; 8·5[b]	505; 417	2·15; 1·77

[a] $\varphi_{EtOH} = 5\%$, [b] $\varphi_{EtOH} = 10\%$.

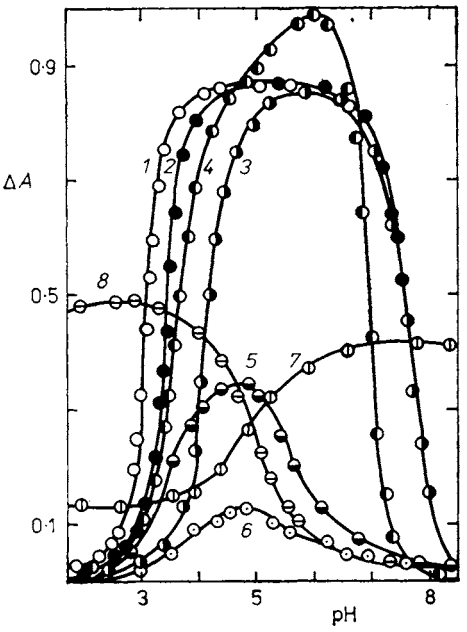

FIG. 10

Absorbance–pH curves of the UO_2^{2+}–CAS–SPX system at 612 nm; $c_M = 7-350$ μmol . l^{-1}, $c_L = 7-49$ μmol l^{-1}, $c_T = 1$ mmol . l^{-1}, $\varphi_{EtOH} = 5\%$. Curves (c_M/c_L): *1* 50·0, *2* 10·0, *3* 1·0, *4* 0·29; UO_2^{2+}–CAS (free from surfactant): *5* 50·0 (592 nm), *6* 0·14 (575 nm); CAS–SPX (c_T/c_L): *7* 41 (420 nm), *8* 41 (520 nm)

previously[24]. With increasing nitrate concentration, λ_{max} 614 nm shifts to 607 nm at $c_{NO_3^-} = 0{\cdot}2$ mol l^{-1}.

UO_2^{2+}–ECR–SPX *Ternary System*

Typical absorption spectra of UO_2^{2+} solutions in the presence of excess reagent and surfactant are reproduced in Fig. 11; they exhibit analogous changes in dependence on pH and concentrations of components as those of the system with CAS. Changes in the positions of the absorption maxima and in the molar absorptivities in dependence on the concentration of UO_2^{2+} and the excess of reagent are given in Table VII. Absorbances at $\lambda > 590$ nm for solutions with excess reagent and pH < 5·6 are only steady after 20 min from the solution mixing. The absorbance–pH curves, measured at $c_M = 7-378$ μmol l^{-1}, $c_L = 7-24{\cdot}5$ μmol l^{-1}, $c_T = 1$ mmol l^{-1}, pH 1·9–8·6, λ 640–400 nm, exhibit two formation ranges, viz. pH 2·0–4·5 and pH 4·5–5·7 for solutions with excess uranium, and four formation ranges for solutions with excess reagent similarly as with CAS, hence, at pH 2·0–4·0, pH 4·0–5·7, pH 5·7–7·0, and pH 7·0–8·6. The characteristic pH ranges, however, are shifted to higher values owing to the higher pK_{a3} value of the reagent.

The absorption spectra in dependence on c_L at pH 5·6 form two defined isosbestic points, at 600 nm for $c_L = 21-35$ μmol l^{-1} and at 585 nm for $c_L = 53-87$ μmol . . l^{-1}. The absorption maximum shifts only slightly, from 595 to 592 nm at $p_L = 12{\cdot}5$, and the molar absorptivity for uranium decreases markedly at $p_L > 7{\cdot}5$. The $\Delta A = f(c_L)$ dependences exhibit a clear-cut plateau in dependence on wavelength. At

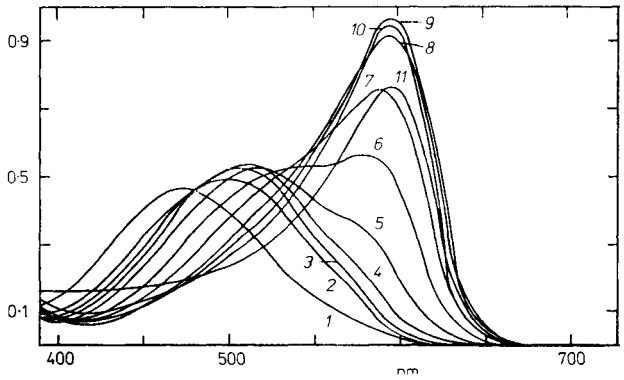

FIG. 11

Absorption spectra of the UO_2^{2+}–ECR–SPX system with excess reagent; $c_M = 9{\cdot}45$ μmol l^{-1}, $c_L = 40$ μmol l^{-1}, $c_T = 0{\cdot}5$ mmol l^{-1}, $\varphi_{EtOH} = 10\%$ ethanol, pH: *1* 1·11, *2* 1·73, *3* 2·23, *4* 2·90, *5* 3·33, *6* 3·80, *7* 4·33, *8* 4·99, *9* 5·61, *10* 6·06, *11* 6·65

585 nm and pH 5·6, the differential absorbance is highest at $p_L = 5·7$, at a higher excess of reagent the usual decrease in absorbance takes place. The absorption curves in dependence on the concentration of surfactant at pH 5·6 also exhibit two isosbestic points, at 575 nm for $c_T = 0·5-3$ mmol l^{-1} and 535 nm for $c_T = 4-8$ mmol l^{-1}. The maximum in the $\Delta A = f(c_T)$ difference dependence is attained at $c_T = 2·5$ mmol l^{-1}. With this reagent the decrease in the absorbances for excess surfactant is less pronounced than with CAS or CAB. The characteristic absorbance curves indicate similar equilibria in solution as with CAS. A drawback of ECR as compared to CAB or CAS is in the considerably lower conditional molar absorptivities of the ternary complexes of uranium and in the instability of the reagent in solution under the conditions that are optimum for the determination of uranium.

Numerical Analysis of Absorbance Curves for the Uranyl–Reagent–Surfactant Ternary Systems Using the SQUAD-G *Program*

The experimental spectrophotometric data from the absorbance–pH curves were treated *a*) for solutions with excess UO_2^{2+}: $c_M = 70-350$ μmol l^{-1}, $c_L = 7$ μmol l^{-1} for systems with CAB and CAS, and $c_M = 378$ μmol l^{-1}, $c_L = 7$ μmol l^{-1} for systems with ECR; *b*) for equimolar solutions: $c_M = c_L = 7$ μmol l^{-1}; and *c*) for solutions with excess reagent: $c_M = 3·5-7$ μmol l^{-1}, $c_L = 7-70$ μmol l^{-1} for systems with CAB, and $c_M = 7$ μmol l^{-1}, $c_L = 24·5$ μmol l^{-1} for systems with CAS or ECR. The concentration of surfactant was $c_T = 0·3-5$ mmol l^{-1} for systems with CAB and 1 mmol l^{-1} for systems with CAS or ECR ($p_{T(L)} = 12·3$ to 204). A total of 19 absorbance–pH curves were processed over the region of pH 2·2 – 6·0 unless displacement of the ternary complex(es) from the space of the micelle and its (their) decomposition to binary associates of the reagent species with the surfactant took place. In the numerical analysis, data from the first formation

TABLE VII

Optical characteristics of the UO_2^{2+}–ECR–SPX system; $\varphi_{EtOH} = 5\%$ or 10%, $I = 0·005$ or 0·1 ($HCl + NH_3$)

c_M μmol l^{-1}	c_L μmol l^{-1}	c_T mmol l^{-1}	pH_{opt}	λ_{max} nm	$\varepsilon_{cond} \cdot 10^{-4}$ l mol^{-1} cm^{-1}
189	7	1·0	5·0	590; 573	7·73; 6·30
9·45	40	0·5	5·6	595	8·99
9·45	40	0	5·5[a]	535	1·45
0	40	0·5	3·0; 9·0[a]	507; 428	2·21; 1·91

[a] $\varphi_{EtOH} = 10\%$, $I = 0·1$.

region of the curves were first processed and data from the second and, where existing, from the third and fourth regions were consecutively added. The individual curves were first treated separately and later together for cases *a*), *b*) and *c*). A number of probable chemical models, emerging as combinations of the chemical equilibria shown below, were tested (these equilibria are for CAB; for CAS and ECR the equilibria were analogous, only the basic H_2L^{2-} species was considered in place of H_2L^-):

$$H_2L \rightleftharpoons HL^{2-} + H^+ \qquad {}^*K_{a3} \qquad (A)$$

$$UO_2^{2+} + H_2L^- \rightleftharpoons UO_2LH_2^+ \qquad {}^*\beta'_{110} \qquad (B)$$

$$UO_2^{2+} + H_2L^- \rightleftharpoons UO_2LH + H^+ \qquad {}^*\beta'_{111} \qquad (C)$$

$$UO_2^{2+} + H_2L^- \rightleftharpoons UO_2L^- + 2\,H^+ \qquad {}^*\beta'_{112} \qquad (D)$$

$$UO_2^{2+} + 2\,H_2L^- \rightleftharpoons UO_2L_2L_2^{2-} + 2\,H^+ \qquad {}^*\beta'_{122} \qquad (E)$$

$$UO_2^{2+} + 2\,H_2L^- \rightleftharpoons UO_2L_2H^{3-} + 3\,H^+ \qquad {}^*\beta'_{123} \qquad (F)$$

$$UO_2^{2+} + 2\,H_2L^- \rightleftharpoons UO_2L_2^{4-} + 4\,H^+ \qquad {}^*\beta'_{124} \qquad (G)$$

$$2\,UO_2^{2+} + H_2L^- \rightleftharpoons (UO_2)_2L^+ + 2\,H \qquad {}^*\beta'_{212} \qquad (H)$$

$$2\,UO_2^{2+} + 2\,H_2L^- \rightleftharpoons (UO_2)_2L_2H_2 + 2\,H^+ \qquad {}^*\beta'_{222} \qquad (I)$$

$$2\,UO_2^{2+} + 2\,H_2L^- \rightleftharpoons (UO_2)_2L_2^{2-} + 4\,H^+ \qquad {}^*\beta'_{224} \qquad (J)$$

$$UO_2^{2+} + H_2O \rightleftharpoons UO_2OH^+ + H^+ \qquad \beta'_{101} \qquad (K)$$

$$2\,UO_2^{2+} + H_2O \rightleftharpoons (UO_2)_2OH^{3+} + H^+ \qquad \beta'_{201} \qquad (L)$$

$$2\,UO_2^{2+} + 2\,H_2O \rightleftharpoons (UO_2)_2(OH)_2^{2+} + 2\,H^+ \qquad \beta'_{202} \qquad (M)$$

$$3\,UO_2^{2+} + 5\,H_2O \rightleftharpoons (UO_2)_3(OH)_5^+ + 5\,H^+ \qquad \beta'_{305} \qquad (N)$$

$$UO_2^{2+} + H_2L^- + H_2O \rightleftharpoons UO_2L(OH)^{2-} + 3\,H^+ \qquad {}^*\beta'_{113} \qquad (O)$$

$$UO_2^{2+} + H_2L^- + 2\,H_2O \rightleftharpoons UO_2L(OH)_2^{3-} + 4\,H^+ \qquad {}^*\beta'_{114} \qquad (P)$$

$$UO_2^{2+} + H_2L^- + 4\,H_2O \rightleftharpoons UO_2L(OH)_4^{5-} + 6\,H^+ \qquad {}^*\beta'_{116} \qquad (Q)$$

$$2\,UO_2^{2+} + H_2L^- + H_2O \rightleftharpoons (UO_2)_2L(OH) + 3\,H^+ \qquad {}^*\beta'_{213} \qquad (R)$$

$$2\,UO_2^{2+} + H_2L^- + 2\,H_2O \rightleftharpoons (UO_2)_2L(OH)_2^- + 4\,H \qquad {}^*\beta'_{214} \qquad (S)$$

$$2\,UO_2^{2+} + 2\,H_2L^- + 2\,H_2O \rightleftharpoons (UO_2)_2L(OH)_2^{4-} + 6\,H^+ \qquad {}^*\beta'_{226} \qquad (T)$$

$$2\,UO_2^{2+} + 3\,H_2L^- \rightleftharpoons (UO_2)_2L_3^{5-} + 6\,H^+ \qquad {}^*\beta'_{236} \qquad (U)$$

$$2\,UO_2^{2+} + 3\,H_2L^- + H_2O \rightleftharpoons (UO_2)_2L_3(OH)^{6-} + 7\,H^+ \qquad {}^*\beta'_{237} \qquad (V)$$

$$2\,UO_2^{2+} + 3\,H_2L^- + 2\,H_2O \rightleftharpoons (UO_2)_2L_3(OH)_2^{7-} + 8\,H^+ \qquad {}^*\beta'_{238} \qquad (W)$$

$$2\,UO_2^{2+} + 3\,H_2L^- + 3\,H_2O \rightleftharpoons (UO_2)_2L_3(OH)_3^{8-} + 9\,H^+ \qquad {}^*\beta'_{239} \qquad (X)$$

$$H_2L^- + T^+ \rightleftharpoons \{H_2L^-, T^+\} \qquad \beta_{LT} \qquad (Y)$$

$$HL^{2-} + 2\,T^+ \rightleftharpoons \{HL^{2-}, 2\,T^+\} \qquad \beta_{LT_2} \qquad (Z)$$

$$H_2L^- \rightleftharpoons HL^{2-} + H^+ \qquad K'_{a3} \qquad (AA)$$

$$UO_2^{2+} + H_2L^- + T^+ \rightleftharpoons \{UO_2L^-, T^+\} + 2\,H^+ \qquad {}^*\beta_{11T} \qquad (BB)$$

$$UO_2^{2+} + 2\,H_2L^- + 4\,T^+ \rightleftharpoons \{UO_2L_2^{4-}, 4\,T^+\} + 4\,H^+ \qquad {}^*\beta_{12T} \qquad (CC)$$

For all absorbance–pH curves the procedure was such that to the starting model in the first formation region, models with additional complexes were tested successively until the best fit to the experimental absorbances was reached. For the model with the best fit, data from the second formation region were added and additional complexes were tested till the best fit, etc. The pK'_{a3} conditional constants of the reagents in the presence of surfactant, stability constants of binary associates with the surfactant (β_{LT} and β_{LT_2}) and molar absorptivities of the acid-base species, calculated previously, were held unaltered during the minimization. For the pH curves of solutions with excess uranium, various combinations of the equilibria (A), (B) to (N) were primarily tested. For the pH curves of equimolar solutions and solutions with excess reagent, combinations of equilibria $(O)-(Z)$, $(AA)-(CC)$ were also tested. The values of the constants for the hydrolysis equilibria $(K)-(N)$[1], which were also held constant during the minimization, were accepted by the SQUAD-G program, no improvement in the fit to the experimental absorbance, however, was thereby achieved. In solutions with a constant concentration of surfactant, the stoichiometric coefficient for the surfactant in the ternary species involving the surfactant was not determined, although such defined ionic associates necessarily exist in the solutions. Interactions of such associates with the surfactant micelle did not manifest themselves. Therefore, the equilibria tested ($(A)-(J)$, $(O)-(X)$) were formulated omitting the surfactant, and the resulting equilibrium constant ${}^*\beta'_{ijk}$ has a conditional character.

The criteria used for adopting a model or for including a species were *a*) convergence of the calculation; *b*) minimal value of the sum of squares of absorbance residuals,

$$U = \sum_{i=1}^{n} (A_{\mathrm{exp},i} - A_{\mathrm{calc},i})^2 , \qquad (1)$$

where n is the total number of absorbance data for all solutions and wavelengths used; *c*) minimal value of the standard deviation of absorbance $s(A)$; *d*) for the standard deviation of the calculated equilibrium constant, validity of the condition

$$s(\log \beta_i) \leqq (1/10) \log \beta_i \,. \qquad (2)$$

The real results of calculations are given in Tables VIII and IX for complexes of CAB and CAS, respectively. In the CAB system with excess uranium ($c_M = 70-350$ μmol . . l^{-1}, $c_L = 7$ μmol l^{-1}) at pH 2·1–4·7 and in the presence of SPX at $c_T = 0{\cdot}1$ mol . . l^{-1}, the best fit was obtained with the model of H_2L^-, HL^{2-}, UO_2L^-, UO_2LH; for solutions with a small excess of reagent ($c_L = 24{\cdot}5$ μmol l^{-1}, $c_M = 7$ μmol l^{-1}) and $c_T = 1$ mmol l^{-1}, pH 2·1–6·0, the model of H_2L^-, HL^{2-}, UO_2L^-, UO_2LH and $UO_2L_2^{4-}$ was adopted; and for solutions with the same c_M and c_L and pH and at surfactant concentrations covering the region of 0·3–5 mmol l^{-1}, the model of H_2L^-, HL^{2-}, $\{H_2L^-, T^+\}$, $\{HL^{2-}, 2\,T^+\}$, $\{UO_2L^-, T^+\}$, $\{UO_2L_2^{4-}, 4\,T^+\}$ was found suitable. For solutions with a tenfold excess of reagent ($c_L = 70$ μmol l^{-1}, $c_M = 7$ μmol l^{-1}) and $c_T = 1$ mmol l^{-1}, the best fit over the same pH range was obtained with the model of H_2L^-, HL^{2-}, UO_2L^-, $UO_2L_2^{4-}$, UO_2LH, $UO_2L_2H_2^{2-}$. For other and additional combinations of complexes UO_2L^-, $(UO_2)_2L(OH)$, $(UO_2)_2L(OH)_2^-$, $UO_2L_2^{4-}$, $UO_2L_2H_2^{2-}$, $UO_2LH_2^+$, $UO_2L(OH)^{2-}$, $(UO_2)_2L_2(OH)_2^{4-}$, $UO_2L_2H^{3-}$, $(UO_2)_2L_3^{5-}$, $(UO_2)_2L_3(OH)^{6-}$, $(UO_2)_2L_3(OH)_2^{7-}$, $(UO_2)_2L_3(OH)_3^{8-}$, $UO_2L(OH)^{2-}$, $UO_2L(OH)^{5-}$ in addition to the H_2L^- and HL^{2-} species in equimolar solutions and in solutions with excess reagent, and for combinations of complexes UO_2L^-, $(UO_2)_2L_2H_2$, $(UO_2)_2L_2^{2-}$, $UO_2L_2H^{3-}$, $UO_2LH_2^+$, $(UO_2)_2L^+$, $UO_2L_2^{4-}$, and $UO_2L_2H_2^{2-}$ in solutions with excess uranium in the above conditions the calculations did not converge or the values of the constants oscillated or the molar absorptivities attained unreasonable values or the standard deviations of the constants and/or the molar absorptivities were too high.

Similarly, for systems with CAS and ECR, the best fit for solutions with excess uranium ($c_M = 70-350$ μmol l^{-1}, $c_L = 7$ μmol l^{-1}, pH 1·9–4·6 for CAS and $c_M = 378$ μmol l^{-1}, $c_L = 7$ μmol l^{-1}, pH 2·5–4·25 for ECR), $c_T = 1$ mmol l^{-1}, was obtained using the model of H_2L^{2-}, HL^{3-}, UO_2L^{2-}, UO_2LH^-; for solutions with a small excess of reagent ($c_L = 24{\cdot}5$ μmol l^{-1}, $c_M = 7$ μmol l^{-1}), pH 2·0–5·9 for CAS and pH 2·5–5·6 for ECR, $c_T = 1$ mmol l^{-1}, the model of H_2L^{2-}, HL^{3-}, UO_2L^{2-}, UO_2LH^-, $UO_2L_2^{6-}$ suits best. For other and additional combinations of complexes, UO_2L^{2-}, $UO_2L_2^{6-}$, $UO_2L(OH)^{3-}$, $UO_2L(OH_2^{4-}$, $(UO_2)_2L_3(OH)_2^{10-}$, $UO_2L_2H_2^{4-}$, UO_2LH^- in solutions with a small excess of reagent in the presence of surfactant, and UO_2L^{2-}, $UO_2L_2^{6-}$, $UO_2L_2H^{5-}$, $UO_2L_2H^{5-}$, $UO_2L_2H_2^{4-}$, $(UO_2)_2L_2H_2^{2-}$, $(UO_2)_2L_2^{4-}$, $(UO_2)_2L$ and UO_2LH in solutions with excess uranium, the calculations gave no reasonable results.

TABLE VIII

Estimation of the chemical model for the UO_2^{2+}–CAB–SPX system by minimization of absorbance–pH curves (28 wavelengths within the 660–400 nm range) by means of SQUAD-G program; $\varphi_{EtOH} = 5\%$, $I = 0{\cdot}05$ (HCl + NH_3)

Assumed species	log $*\beta'$ (cond.)	$\bar{\varepsilon} \cdot 10^{-4}$ (λ, nm) l mol^{-1} cm^{-1}	$s(A)$	U
$c_M = 350$ μmol l^{-1}, $c_L = 7$ μmol l^{-1}, $c_T = 1$ mmol l^{-1}, pH 2·15–4·53 (21 values)				
H_2L^-, HL^{2-}	—	—	0·033	0·603
UO_2L^-	−2·72 ± 0·01	13·1 (635)		
H_2L^-, HL^{2-}	—	—		
UO_2L^-	−2·73 ± 0·01	13·0 (635)		
$UO_2(OH)^+$, $(UO_2)_2(OH^{3+}$	—	—	0·033	0·609
$(UO_2)_2(OH)_2^{2+}$, $(UO_2)_3(OH)_5^+$	—	—		
$c_M = 350$ and 189 and 70 μmol l^{-1}, $c_L = 7$ μmol l^{-1}, $c_T = 1$ mmol l^{-1}, pH 2·15–4·73 (61 values)				
H_2L^-, HL^{2-}	—	—		
UO_2L^-	−2·52 ± 0·01	15·1 (635)	0·017	0·170
UO_2LH	0·76 ± 0·03	5·01 (610)		
$c_M = 7$ μmol l^{-1}, $c_L = 7$ μmol l^{-1}, $c_T = 1$ mmol l^{-1}, pH 2·82–5·66 (21 values)				
H_2L^-, HL^{2-}	—	—	0·020	0·177
UO_2L^-	−2·58 ± 0·03	9·70 (630)		
H_2L^-, HL^{2-}	—	—		
UO_2L^-	−2·36 ± 0·04	14·3 (635)	0·012	0·101
UO_2LH	0·69 ± 0·05	4·51 (610)		
$c_M = 7$ μmol l^{-1}, $c_L = 24{\cdot}5$ μmol l^{-1}, $c_T = 1$ mmol l^{-1}, pH 2·17–4·07 (14 values)				
H_2L^-, HL^{2-}	—	—	0·022	0·165
UO_2L^-	−2·05 ± 0·02	12·9 (625)		
Concentrations as above, pH 2·17–5·82 (25 values)				
H_2L^-, HL^{2-}	—	—	0·011	0·100
UO_2L^-	−2·05 ± 0·01	13·2 (630)		
$UO_2L_2^{4-}$	−6·25 ± 0·03	11·6 (616)		
H_2L^-, HL^{2-}	—	—		
UO_2L^-	−2·26 ± 0·01	14·5 (635)	0·009	0·043
$UO_2L_2^{4-}$	−6·25 ± 0·05	11·7 (615)		
UO_2LH	0·76 ± 0·05	5·01 (610)		

TABLE VIII
(*Continued*)

Assumed species	log *β′ (cond.)	$\bar{\varepsilon} \cdot 10^{-4}$ (λ, nm) l mol^{-1} cm^{-1}	s(A)	U
Concentrations as above[a], pH 2·39—9·55 (39 values)				
H_2L^-, HL^{2-}	—	—		
UO_2L^-	−2·31 ± 0·01	13·8 (630)	0·017	0·298
$UO_2L_2^{4-}$	−5·70 ± 0·04	9·60 (620)		
$UO_2L(OH)_2^{3-}$	−17·05 + 0·06	3·41 (535)		
c_M = 3·5 μmol l^{-1}, c_L = 14 μmol l^{-1}, c_T = 1 mmol l^{-1}, pH 2·32—4·05 (12 values)				
H_2L^-, HL^{2-}	—	—		
UO_2L^-	−2·25 ± 0·02	12·2 (625)	0·003	0·002
UO_2LH	0·29 ± 0·09	6·01 (610)		
c_M = 7 μmol l^{-1}, c_L = 70 μmol l^{-1}, c_T = 1 mmol l^{-1}, pH 2·01—5·20 (21 values)				
H_2L^-, HL^{2-}	—	—		
UO_2L^-	−2·30 ± 0·02	13·7 (635)	0·007	0·025
$UO_2L_2^{4-}$	−6·24 ± 0·05	10·7 (615)		
UO_2LH	−0·71 ± 0·05	4·62 (610)		
H_2L^-, HL^{2-}	—	—		
UO_2L^-	−2·35 ± 0·03	13·9 (635)	0·006	0·015
$UO_2L_2^{4-}$	−6·31 ± 0·06	11·6 (615)	0·006	0·015
UO_2LH	0·63 ± 0·06	4·65 (610)		
$UO_2L_2H_2^{2-}$	2·37 ± 0·06	6·14 (610)		
c_M = 7 μmol l^{-1}, c_L = 24·5 μmol l^{-1}, c_T = 1 mmol l^{-1}, pH 2·77—5·82 (25 values)				
H_2L^-, HL^{2-}	—	—		
$\{H_2L^- . T^+\}$, $\{HL^{2-}, 2\,T^+\}$	—	—	0·011	0·108
UO_2LT	2·88 ± 0·05	13·5 (630)		
$UO_2L_2T_4$	8·71 ± 0·12	11·2 (615)		
Concentrations as above, C_T = 0·3—5 mmol l^{-1}, pH 2·11—5·82 (70 values)				
H_2L^-, HL^{2-}	—	—		
$\{H_2L^-, T^+\}$, $\{HL^{2-}, 2\,T^+\}$	—	—		
UO_2LT	3·15 ± 0·04	13·7 (635)	0·012	0·110
$UO_2L_2T_4$	8·36 ± 0·27	11·5 (615)		

[a] I = 0·05 (HNO_3 + NH_3).

TABLE IX

Estimation of the chemical model for the UO_2^{2+}–CAS–SPX system by minimization of absorbance–pH curves (28 wavelengths within the 645–400 nm range) by means of SQUAD-G program; $\varphi_{EtOH} = 5\%$), $I = 0{\cdot}05$ (HCl + NH_3)

Assumed species	$\log {}^*\beta'$ (cond.)	$\bar{\varepsilon} \cdot 10^{-4}$ (λ, nm) l mol^{-1} cm^{-1}	$s(A)$	U
$c_M = 350$ μmol l^{-1}, $c_L = 7$ μmol l^{-1}, $c_T = 1$ mmol l^{-1}, pH 1·91–4·65 (20 values)				
H_2L^{2-}, HL^{3-}	—	—		
UO_2L^{2-}	−2·70 ± 0·01	12·25 (615)	0·013	0·103
H_2L^{2-}, HL^{3-}	—	—		
UO_2L^{2-}	−2·70 ± 0·01	12·3 (615)		
$UO_2(OH)^+$, $(UO_2)_2(OH)^{3+}$	—	—	0·014	0·108
$(UO_2)_2(OH)_2^{2+}$, $(UO_2)_3(OH)_5^+$	—	—		
$c_M = 350$ μmol l^{-1} and 70 μmol l^{-1}, $c_L = 7$ μmol l^{-1}, $c_T = 1$ mmol l^{-1}, pH 1·91–4·65 (38 values)				
H_2L^{2-}, HL^{3-}	—	—	0·012	0·092
UO_2L^{2-}	−2·71 ± 0·01	12·4 (615)		
H_2L^{2-}, HL^{3-}	—	—		
UO_2L^{2-}	−2·67 ± 0·04	12·25 (615)	0·010	0·052
UO_2LH	0·58 ± 0·06	5·85 (590)		
$c_M = c_L = 7$ μmol l^{-1}, $c_T = 1$ mmol l^{-1}, pH 2·63–5·66 (22 values)				
H_2L^{2-}, HL^{3-}	—	—	0·012	0·098
UO_2L^{2-}	−2·80 ± 0·01	12·83 (615)		
H_2L^{2-}, HL^{3-}	—	—		
UO_2L^{2-}	−2·71 ± 0·02	12·70 (615)	0·009	0·038
UO_2LH^-	0·29 ± 0·09	5·57 (590)		
$c_M = 7$ μmol l^{-1}, $c_L = 24{\cdot}5$ μmol l^{-1}, $c_T = 1$ mmol l^{-1}, pH 2·03–5·88 (25 values)				
H_2L^{2-}, HL^{3-}	—	—	0·023	0·368
UO_2L^{2-}	−2·55 ± 0·01	12·52 (615)	0·023	0·368
H_2L^{2-}, HL^{3-}	—	—		
UO_2L^{2-}	−2·50 ± 0·01	11·11 (610)	0·009	0·055
$UO_2L_2^{6-}$	−7·07 ± 0·04	14·24 (615)		
H_2L^{2-}, HL^{3-}	—	—		
UO_2L^{2-}	−2·50 ± 0·02	12·10 (615)	0·005	0·015
$UO_2L_2^{6-}$	−7·02 ± 0·05	14·16 (615)		
UO_2LH^-	0·39 ± 0·06	6·05 (590)		

DISCUSSION

This study gave evidence that in solutions of UO_2 with triphenylmethane dyes with the functional-analytical group of salicylic acid, defined equilibria establish also at micellar or submicellar concentrations of a cationic surfactant, various ternary complexes being formed in dependence on the concentrations of the reactants and on pH.

In solutions with a concentration excess of uranium ($c_M = 70-380\ \mu mol\ l^{-1}$, $c_L = 7\ \mu mol\ l^{-1}$) at $c_T = 1\ mmol\ l^{-1}$ and pH 2–5, a ternary complex with the stoichiometric ratio of the components M : L : T = 1 : 1 : 1 is formed, viz.

$$UO_2^{2+} + \{H_2L^-, T^+\} \rightleftharpoons \{UO_2L^-, T^+\} + 2\,H^+ \qquad (DD)$$

for CAB, and

$$UO_2^{2+} + \{H_2L^{2-}, 2\,T^+\} \rightleftharpoons \{UO_2L^{2-}, 2\,T^+\} + 2\,H^+ \qquad (EE)$$

for CAS and ECR. The formation of these complexes was proved unambiguosly by numerical analysis of spectrophotometric data as well as by graphical analysis of absorbance–pH curves and by the corresponding solutions and continuous variations methods[17,24]. The complexes formed are characterized by the long-wavelength absorption maxima, the high molar absorptivities and the high colour contrast n comparison to the reagent–surfactant binary system ($\Delta\lambda_{max}$ = 123, 106, and 83 nm or CAB, CAS, and ECR, respectively). Supposing a simple structure (Scheme 3)

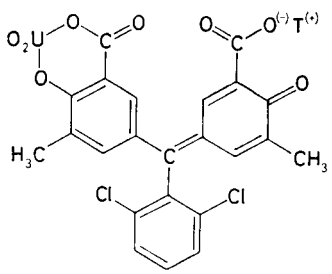

$UO_2L^-\,T^+$

SCHEME 3

the useful optical properties of the complex can be explained by an increased electron-pair delocalization on the functional oxygen atom, after the phenolic proton has been dissociated more easily in the presence of the adjacent surfactant (bound) and in micellar medium with decreased water concentration.

The analogous complexes with CAS and ECR only differ in the bonding of the second molecule of surfactant at the SO_3^- group of the reagent in position 3 in the $\{H_2L^{2-}, 2\,T^+\}$ species. Analogous composition is assumed for the low-soluble ionic associate, which is formed under the same conditions in solutions with a stoichiometric concentration of surfactant ($c_T \approx 0{\cdot}1$ mmol l^{-1}). With increasing concentration of the cationic surfactant, this associate is first solubilized without changes in the optical properties. In solutions at above-critical concentrations of surfactant, the ternary complex interacts with the surface of the micelle or is extracted into the micelle whereupon the short-wavelength component of the absorption double maximum increases on the expense of the long-wavelength component; this results, e.g., in a decrease in molar absorptivities at 635 and 612 nm for the CAB and CAS complexes, respectively. A cause of this may be an altered permittivity of medium or increased interaction of the ternary complex with the electric field of the micelle.

Numerical data analysis, however, also revealed that in equimolar solutions and in solutions with excess reagent or uranyl, a small amount of a different complex with the M : L : T = 1 : 1 : 1 is also formed, a single proton being split off from the H_2L species. In this case the phenolic proton is not split off during the reagents reaction with uranyl; the complex exhibits its absorption maximum at considerably shorter wavelengths and the molar absorptivity is lower (Table X and Scheme 4).

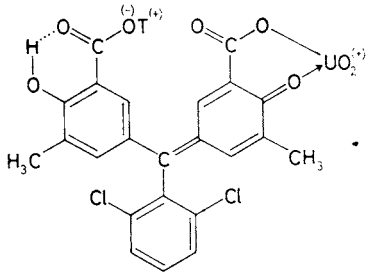

UO_2LH,T^+

SCHEME 4

During the reaction with CAB, the $\{UO_2LH^-, T^+\}$ complex is formed at pH 2–4, $c_L = 7-70$ μmol l^{-1}, $c_M = 3{\cdot}5-7$ μmol l^{-1}, $c_T = 1$ mmol l^{-1}. The occurrence of this complex, little absorbing in the long-wavelength spectral region, was also confirmed by the corresponding solutions method for excess reagent, $p_L = 1{\cdot}0-3{\cdot}5$ (the ratio of the amount of reagent substance to the amountof substance of split-off protons was 0·85 for CAB and 9·65 for CAS), as well as by the continuous variations method at pH 4, λ 620–650 nm, $c_T = 0{\cdot}3-2$ mmol l^{-1}. In solutions with variable concentrations of surfactant, a smooth transition between the two

complexes with the M : L : T = 1 : 1 : 1 ratio takes place. Formation of two different complexes with the stoichiometric ratio M : L = 1 : 1, exhibiting different optical properties, was also found for CAS in aqueous solutions free from surfactant, namely, when comparing solutions with excess uranyl ($p_M = 50$, λ_{max} 592 nm, $\varepsilon = 4{\cdot}85 \cdot 10^4$ l mol^{-1} cm^{-1}) and solutions with a small excess of reagent ($p_L = 7$, λ_{max} 575 nm, $\varepsilon = 1{\cdot}73 \cdot 10^4$ l mol^{-1} cm^{-1}). The preferential formation of the complex with structure *II* without surfactant in acid solution is probably due to a shielding of the quinoid oxygen by proton in the H_3L^- species, which prevails in this medium[6].

In solutions with excess CAB ($p_L = 2-10$, $c_L = 14-70$ μmol l^{-1}) at $c_T = 0{\cdot}3$ to 5 mmol l^{-1} and pH 4·0–5·9, numerical analysis gave evidence that a second molecule of the reagent is also bonded to the uranyl, four protons being split off. Bonding of additional molecules of tenside is likely, and the $\{UO_2L_2T_2^{2-}, 2\,T^+\}$ ternary complex formed passes into the micellar phase. The M : L = 1 : 2 ratio in the complex was also confirmed by the continuous variations method at a constant concentration of tenside ($x_L = c_L/(c_L + c_M) = 0{\cdot}63$ at pH 5·75). Analogous complexes are also formed with CAS at pH 4·0–6·1 (see also ref.[24]) and with ECR at pH 4·0–5·7, and these differ from the complex with CAB only in the presence of an additional molecule of surfactant associated to SO_3^-, which, however, does not affect the optical properties of the complex. Molar absorptivity of the formed complex with the M : L = 1 : 2 ratio by far does not reach the double value of that of $\{UO_2L^-, T^+\}$ for CAB or $\{UO_2L^{2-}, 2\,T^+\}$ for CAS and ECR; at some wavelengths it is even lower (Table X). The number of detached protons gives evidence of bonding of the phenolic hydroxy and carboxy groups in each molecule of the reagent, thus eliminating the possibility of occurrence of internally polyfunctionally bonded uranium. The different optical properties of the UO_2LT and $\{UO_2L_2^{4-}, 4\,T^+\}$

TABLE X

Values of λ_{max}(nm) and $\bar{\varepsilon}$(l mol^{-1} cm^{-1}) of complexes in the uranyl–reagent–Septonex^R systems

Complex	CAB		CAS		ECR	
	λ_{max}	$\bar{\varepsilon} \cdot 10^{-4}$ [a]	λ_{max}	$\bar{\varepsilon} \cdot 10^{-4}$	λ_{max}	$\bar{\varepsilon} \cdot 10^{-4}$ [a]
$\{UO_2L^-, T^+\}$	635	15·10	—	—	—	—
$\{UO_2LH, T^+\}$	610	5·01	—	—	—	—
$\{UO_2L_2^{4-}, 4\,T^+\}$	617	11·80	—	—	—	—
$\{UO_2L_2H_2^{2-}, 2\,T^+\}$	610	6·13	—	—	—	—
$\{UO_2L^{2-}, 2\,T^+\}$	—	—	614	12·30	590	6·59
$\{UO_2LH^-, 2\,T^+\}$	—	—	590	6·05	550	4·30
$\{UO_2L_2^{6-}, 6\,T^+\}$	—	—	612	14·30	593	9·49

[a] Average values.

complexes are due to the difference between the two structures where UO_2^{2+} is bonded in different ways. In solution with a higher excess of reagent ($p_L = 10$, $c_L = 70$ μmol . $.l^{-1}$) at pH 3–5, numerical analysis revealed the occurrence of an additional complex with M : L = 1 : 2, formed with the detachment of two protons, viz. $\{UO_2L_2H_2^{2-}, 2\,T^+\}$, exhibiting a considerably lower molar absorptivity (Table X). In solutions of UO_2^{2+} with excess CAS and free from surfactant, formation of the complex with the M : L = 1 : 2 ratio has not been proved unambiguously[6].

With increasing concentration of reagent at pH 2–6 and a constant concentration of surfactant, in addition to the formation of the ternary complex with M : L = 1 : 1, surfactant is displaced competitively from the complexes and stable binary associates, viz. $\{H_2L^-, T^+\}$ with CAB and $\{H_2L^{2-}, 2\,T^+\}$ with CAS and ECR, arise and displace the ternary complexes from the surface of the micelle into the solution bulk, whereupon these ternary complexes decompose. As a consequence, the molar absorptivity decreases considerably and the absorption maximum shifts to shorter wavelengths. A similar situation also takes place with increasing concentration of surfactant at a constant concentration of reagent: interaction of the ternary complexes, $\{UO_2L^-, T^+\}$ and $\{UO_2L_2^{4-}, 4\,T^+\}$ for CAB and $\{UO_2L^{2-}, 2\,T^+\}$ and $\{UO_2L_2^{6-}, 6\,T^+\}$ for CAB and ECR, with the micelles is first favoured and small optical changes occur; at high concentrations of surfactant the ternary complexes are decomposed, though more slowly, and the above binary associates are formed.

At pH 6–8, the ternary systems exhibit a decrease in absorbance at $\lambda > 575$ nm with time, due to the decomposition of the uranyl–reagent–surfactant complexes to ternary hydrolysis products of unknown composition associated with the detachment of one molecule of reagent, and to $\{HL^{2-}, 2\,T^+\}$ (CAB) or $\{HL^{3-}, 3\,T^+\}$ (CAS, ECR) binary associates. In nitrate medium, where the ternary complexes with surfactant are more stable at pH > 6, the occurrence of a red hydrolytic complex with the M : L = 1 : 1 ratio (λ_{max} 535 nm, $\varepsilon = 3{\cdot}415 \,.\, 10^4$ l mol^{-1} cm^{-1}, equilibrium (*P*)) emerged from the numerical analysis of the absorbance–pH curves for CAB. At pH 8–10 the last molecule of the reagent splits off from the complexes, and the absorbances obtained in the ternary system with surfactant at pH < 10 are virtually identical with those of the reagent–surfactant binary associates. This gives evidence that under these conditions, the solutions only contain reagent–surfactant binary associates in mixtures with hydrolytic complexes of uranyl stabilized at the surfactant micelles.

The equilibrium constants for the observed ternary complexes and those calculated for the chemical models giving the best fit are summarized in Table XI. Distribution diagrams of the complex species in the ternary systems, calculated by the SQUAD-G program from the constants obtained for solutions with excess uranyl or reagent, are shown in Fig. 12, absorption spectra of the individual species calculated by this program are shown in Fig. 13. The contributions from the individual species to the total absorbances over the 660–400 nm region at pH 2–6, calculated by the

SQUAD-G program and drawn by the Digigraph 1 612 device using the adapted PLOT 3D program are shown in Fig. 14 for the UO_2^{2+}–CAB–SPX system at c_M = = 7 μmol l^{-1}, c_L = 24·5 μmol l^{-1}, c_T = 1 mmol l^{-1}. Fig. 14*a* corresponds to the spatial diagram of the composed spectra in dependence on pH. The other spectra sets correspond to the individual components of the system, viz. $\{H_2L^-, T^+\}$, $\{HL^{2-}, 2\,T^+\}$, $\{UO_2L^-, T^+\}$, $\{UO_2L_2^{4-}, 3\,T^+\}$, and $\{UO_2LH^-, T^+\}$. It follows from a comparison of the composed spectrum with the partial spectra that the contributions from the $\{UO_2L_2^{4-}, 4\,T^+\}$ species are substantial from the spectrophotometric point of view. For the two other reagents the situation is analogous.

Complex Equilibria and Optimum Conditions for the Spectrophotometric Determination of Uranium

Out of the observed complexes with CAB, the $\{UO_2L^-, T^+\}$ ternary complex stabilized at the micelles of the surfactant is the most suitable basis for the spectrophotometric determination of uranium. In solutions with excess reagent at pH > 4 and at the micellar concentration of Septonex^R, however, this complex transforms readily into the predominating $\{UO_2L_2T_2^{2-}, 2\,T^+\}$ complex; and only for the CAS and ECR reagents, the analogous $\{UO_2L_2T_4^{2-}, 2\,T^+\}$ complex possesses a molar absorptivity (at λ_{max}) higher than the UO_2LT_2 complex. The actual state is highly dependent on pH, concentrations of reagent and surfactant and also on the concentration of uranium at a given pH. Strictly speaking, to each concentration of uranium (or a narrow concentration region) corresponds an optimum concentration of reagent and an optimum concentration of cationic surfactant and pH, and at other concentrations of uranium this combination of concentrations of reagent and surfactant and pH is no more optimum; the absorptivity decreases. This results

TABLE XI

Average equilibrium constants and their standard deviations for uranyl–reagent complexes in micellar medium of Septonex^R, c_T = 0·3–5 mmol l^{-1}; all results obtained by the SQUAD-G program were used for evalution

Complex	*ijk*	log $*\beta_{ijk}$		
		CAB	CAS	ECR
UO_2L	112	−2·52 ± 0·01	−2·67 ± 0·04	−3·00 ± 0·09
UO_2LH	111	0·76 ± 0·03	0·58 ± 0·06	0·30 ± 0·09
UO_2L_2	124	−6·36 ± 0·06	−7·02 ± 0·05	−6·53 ± 0·05
$UO_2L_2H_2$	122	2·37 ± 0·05	—	—

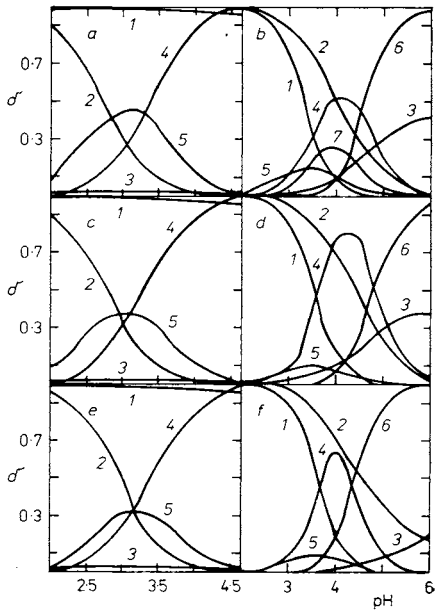

FIG. 12

Distribution diagrams of species in uranyl–reagent–Septonex^R systems. $\varphi_{EtOH} = 5\%$; reagent, c_M (μmol l^{-1}), c_L (μmol l^{-1}), c_T (mmol l^{-1}): *a* CAB, 350, 7·0, 1·0; *b* CAB, 7·0, 24·5, 1·0; *c* CAS, 350, 7·0, 1·0; *d* CAS, 7·0, 24·5, 1·0; *e* ECR, 378, 7·0, 1·0; *f* ECR, 7·0, 24·5, 1·0. Curves: *1* $[UO_2^{2+}]/c_M$, *2* $[H_2L]/c_L$, *3* $[HL]/c_L$, *4* $[UO_2L]/c_M$, *5* $[UO_2LH]/c_M$, *6* $[UO_2L_2]/c_M$, *7* $[UO_2L_2H_2]/c_M$; all species associated with surfactant

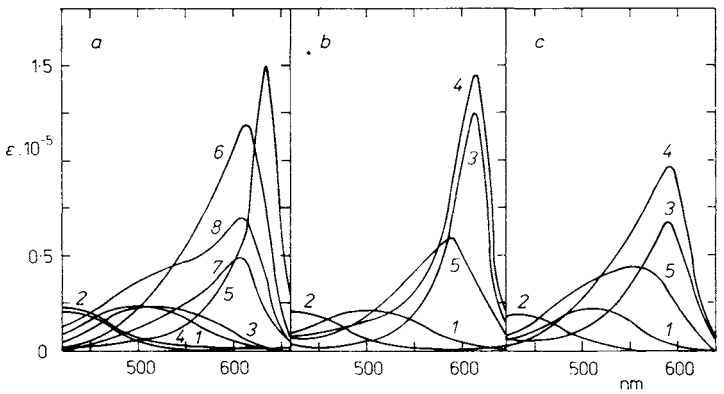

FIG. 13

Calculated spectra of species in uranyl–reagent–Septonex^R systems. *a* CAB, curves: *1* H_2L, *2* HL^{2-}, *3* $\{H_2L^-, T^+\}$, *4* $\{HL^{2-}, 2T^+\}$, *5* $\{UO_2L^-, T^+\}$, *6* $\{UO_2L_2^{4-}, 4T^+\}$, *7* $\{UO_2LH, T^+\}$, *8* $\{UO_2L_2H_2^{2-}, 2T^+\}\}$; *b* CAS; *c* ECR, curves: *1* $\{H_2L^{2-}, 2T^+\}$, *2* $\{HL^{3-}, 3T^+\}$, *3* $\{UO_2L^{2-}, 2T^+\}$, *4* $\{UO_2L_2^{6-}, 6T^+\}$, *5* $\{UO_2LH^-, T^+\}$. Molar absorptivities are in l mol^{-1} cm^{-1}

in distorted calibration plots, lower conditional molar absorptivities and changes in positions of the absorption maxima. For the UO_2^{2+}–CAB–SPX system at the optimum concentrations of $c_L = 10\ \mu mol\ l^{-1}$ and $c_T = 0{\cdot}8\ mmol\ l^{-1}$, the conditional absorptivity increases smoothly with increasing concentration of uranium while the absorption maximum shifts from 617 to 635 nm, which is indicative of the complex with structure *II*. The value of λ_{max} 617 nm indicates the occurrence of a mixture of the $\{UO_2L_2^{4-}, 4\,T^+\}$ and $\{UO_2L_2H_2^{2-}, 2\,T^+\}$ complexes, possessing lower molar absorptivities. The transition between the regions of predominating occurrence of either of the two complexes is characterized by an isosbestic point

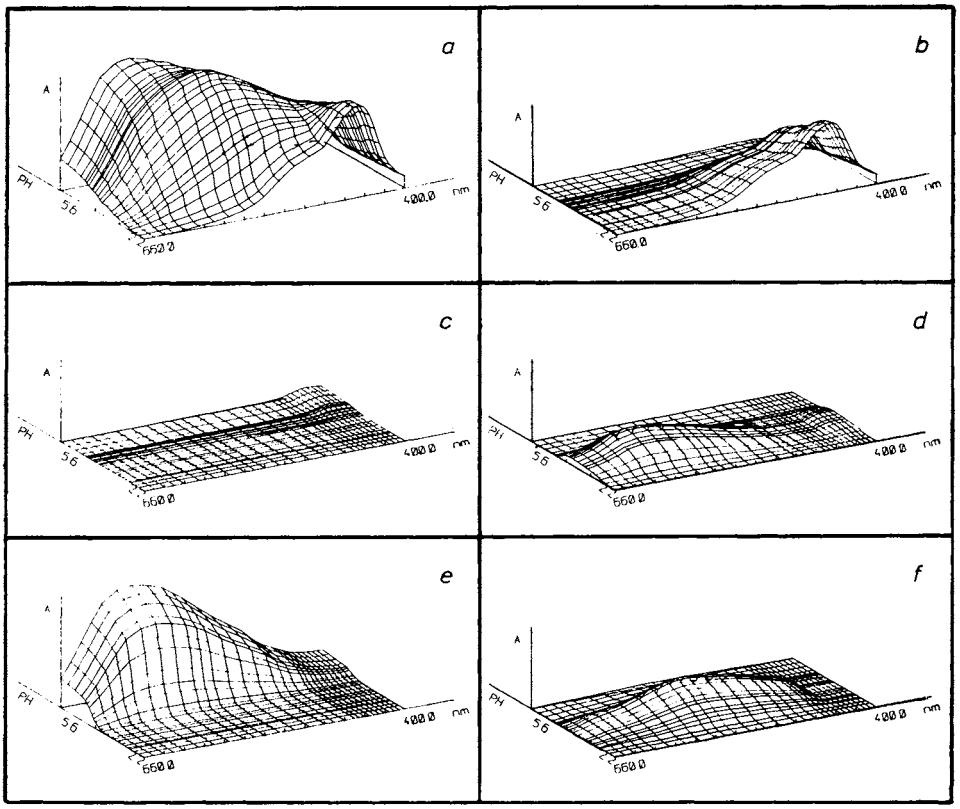

FIG. 14

Spatial diagrams of spectra in dependence on pH; contributions of species to the total absorbance of the UO_2^{2+}–CAB–SPX system. $c_M = 7\ \mu mol\ l^{-1}$, $c_L = 24{\cdot}5\ \mu mol\ l^{-1}$, $c_T = 1\ mmol\ l^{-1}$. *a* experimental spectra, *b* $\{H_2L^-, T^+\}$, *c* $\{HL^{2-}, 2\,T^+\}$, *d* $\{UO_2L^-, T^+\}$, *e* $\{UO_2L_2^{4-}, 4\,T^+\}$, *f* $\{UO_2LH, T^+\}$

at 510 nm. Therefore, this dependence for λ 635 nm is bent at $c_M \leqq 1{\cdot}5$ μmol l^{-1}. For λ 610–625 nm (which is the λ_{max} range for complexes with M : L = 1 : 2), on the other hand, the curves become linear, the molar absorptivity, however, decreases. The calibration plots for solutions with $c_T = 1-2{\cdot}5$ mmol l^{-1} also become linear and their slope decreases, this, however, is a consequence of the partial decomposition of the ternary complexes involving the surfactant. A similar linearization of calibration plots is also achieved for higher concentrations of reagent, particularly at 610–625 nm, because only the $[UO_2L_2^{4-}, 4\,T^+]$ and $[UO_2L_2H_2^{2-}, 2\,T^+]$ species participate; molar absorptivity, however, is lower (Fig. 7). The optimum calibration plots using the three reagents in the presence of a cationic surfactant actually emerge as a compromise of a number of factors including sensitivity of the method, linearity of the plot over a desired region of uranium concentrations, time stability of absorbance and reproducibility of determination.

With CAS and ECR the effect of concentrations of the reagent and surfactant as well as the changes in λ_{max} and conditional molar absorptivities are less marked than with CAB, and as a consequence, the calibration plots are linear over considerably wider regions of uranium concentrations.

The optimum conditions for the determination of uranium using Septonex^R as the surfactant, 0·1M pyridine buffer and medium of 5% (v/v) ethanol at $I = 0{\cdot}05$ are as follows:

For CAB, the study of the reaction mechanism and single-factorial optimization led to pH 5·6, $c_L = 10$ μmol l^{-1}, $c_T = 0{\cdot}8$ mmol l^{-1} for the region of $c_M = 0{\cdot}5$ to

TABLE XII

Optimized conditions and parameters of calibration dependences for the determination of uranium; $\varphi_{EtOH} = 5\%$, $I = 0{\cdot}05$ (HCl + NH_3), pH 5·6 (upper rows); 0·1M pyridine buffer (lower rows)

Reagent	c_T	$(c_M)_{opt}$	λ	$\varepsilon \cdot 10^{-4}$	A_o[a]		c_{lim}[b]
c_L μmol l^{-1}	mmol l^{-1}	μmol l^{-1}	nm	l mol^{-1} cm^{-1}	exp.	calc.	μg ml^{-1}
CAB	0·8	1·5–9	635	14·36 ± 0·12	0·010	−0·063	0·032
10				14·15 ± 0·10	0·162	0·152	0·037
CAS	1·25	0·5–9	612[c]	14·76 ± 0·20	0·023	0·017	0·024
25				14·76 ± 0·21	0·023	0·017	0·017
ECR	2·0	0·5–10	595	9·17 ± 0·08	0·092	0·097	0·041
40				9·17 ± 0·08	0·098	0·099	0·037

[a] Absorbance axis intercept; [b] $c_{lim} = 10s_o \cdot 1\,000M_r/\varepsilon$, where M_r is relative atomic mass, s_o was found from 10 replicate determinations on blank solutions; [c] pH 6.

9 μmol l^{-1}, λ 635 nm; three-factorial and two-factorial simplex processing gave pH 5·6, c_L = 12·3 μmol l^{-1}, c_T = 0·764 mmol l^{-1} for c_M = 8·08 μmol l^{-1}, or c_L = = 15 μmol l^{-1}, c_T = 0·567 mmol l^{-1}, c_M = 7 μmol l^{-1}.

For CAS, the optimum conditions are pH 6·0, c_L = 25 μmol l^{-1}, c_T = 1·25 mmol . . l^{-1}, c_M = 0·5–9·0 μmol l^{-1}, λ 612 nm.

For ECR, the conditions are pH 5·6, c_L = 40 μmol l^{-1}, c_T = 2 mmol l^{-1}, c_M = = 0·5–10 μmol l^{-1}, λ 595 nm.

At other concentrations of reagent and/or tenside, the conditional molar absorptivity is lower, the sensitivity of the method is poorer. Some data are given in Table XII.

The optimum conditions for the spectrophotometric determination of uranium in pure solutions and in chloride medium found by a detailed study of the reaction mechanism were confirmed by consecutive one-factorial optimization as well as by two-factorial and three-factorial simplex processing[53,54] for selected concentrations of uranium and suitably chosen regions of the variable factors. The simplex method, though, can fail to find the reaction optimum if the treatment is brought to a different reaction mechanism in the system by expansion. Changes in the factor levels have to be chosen with circumspection because small changes make the route to the optimum too slow whereas large changes and, in particular, expansion can lead to a false optimum or go astray altogether.

Conditions for the spectrophotometric determination of uranium with CAB, CAS or ECR can be affected considerably by the kind of buffer and agents used for masking interfering ions. A detailed analysis of the problem of spectrophotometric determination of uranium with CAB and CAS in the presence of Septonex^R and application thereof to drinking water and waste-waters will be presented elsewhere.

Thanks are due to Dr M. Souček from the Institute of Organic Chemistry and Biochemistry, Czechoslovak Academy of Sciences, and to Dr F. Vláčil from Department of Analytical Chemistry, Prague Institute of Chemical Technology, for their comments.

REFERENCES

1. Havel J., Sommer L.: Folia Fac. Sci Nat. Univ. Purk. Brun. *14*, Chemia 9, Part 12 (1973).
2. Dey A. K.: Mikrochim. Acta *1958*, 736.
3. Srivastava S. C., Dey A. K.: Inorg. Chem. *2*, 216 (1963).
4. Sinha S. N., Dey A. K.: Indian J. Chem. *1*, 70 (1963).
5. Mukherji A. K., Dey A. K.: J. Inorg. Nucl. Chem. *6*, 314 (1958).
6. Chiacchierini E., Šepel T., Sommer L.: Collect. Czech. Chem. Commun. *35*, 794 (1970).
7. Katsube Y., Uesugi K., Yoe J. H.: Bull. Chem. Soc. Jpn. *34*, 826 (1961).
8. Qureshi S. Z., Bansel R., Anwar K.: Anal. Lett. *17*, 1487 (1984).
9. Tikhonov V. N., Lukina E. V.: Zh. Anal. Khim. *39*, 1646 (1984).
10. Dey A. K., Srivastava S. C., Sángal S. P.: *Proc. 7th Int. Conf. Coord. Chem., Stockholm and Uppsala 1962*; p. 330.
11. Dey A. K.: Mikrochim. Acta *1964*, 414.

12. Tikhonov V. N., Fedotova N. S.: Zh. Anal. Khim. *37*, 1888 (1982).
13. Tikhonov V. N.: Zh. Anal. Khim. *37*, 1960 (1982).
14. Pilipenko A. T., Tananaiko M. M.: *Raznoligandnye i raznometal'nye kompleksy i ikh primenenie v analiticheskoi khimii*, p. 113. Khimiya, Moscow 1983.
15. Marczenko Z.: CRC Crit. Rev. Anal. Chem. *12*, 195 (1981).
16. Parimucha F., Rostek J.: Radioisotopy *11*, 865 (1970).
17. Pištělka M., Stojek B., Havel J.: Collect. Czech. Chem. Commun. *49*, 1974 (1984).
18. Leong C. L.: Anal. Chem. *45*, 201 (1973).
19. Evtimova B.: Anal. Chim. Acta *83*, 397 (1976).
20. Malaník V., Malát M.: Collect. Czech. Chem. Commun. *41*, 42 (1976).
21. Shijo Y., Takeuchi T.: Bunseki Kagaku *20*, 297 (1971); Anal. Abstr. *23*, No. 1, 162 (1772).
22. Kumar S., Kant R., Prakash O.: Rev. Roum. Chim. *29*, 383 (1984).
23. Škrdlík M., Havel J., Sommer L.: Chem. Listy *63*, 939 (1969).
24. Kanický V., Havel J., Sommer L.: Collect. Czech. Chem. Commun. *45*, 1525 (1980).
25. Prakash O., Malát M., Čermáková L.: Collect. Czech. Chem. Commun. *43*, 2536 (1978).
26. Vaňková A.: *Thesis*. Purkyně University, Brno 1983.
27. Otomo M., Kodama K.: Bunseki Kagaku *20*, 1581 (1971); Anal. Abstr. *22*, No. 1, 84 (1972).
28. Jančář L., Havel J.: Scr. Fac. Sci. Nat. Univ. Purk. Brun. *14*, No. 3—4 (Chemia), 73 (1984).
29. Meloun M., Havel J.: Folia Fac. Sci. Nat. Univ. Purk. Brun. *25*, Chemia 17, Part 7 (1984).
30. Jančář L.: *Thesis*. Purkyně University, Brno 1985.
31. Mouková N., Kubáň V., Sommer L.: Chem. Listy *73*, 1106 (1979).
32. Pollaková N., Gotzmannová D., Kubáň V., Sommer L.: Collect. Czech. Chem. Commun. *46*, 354 (1981).
33. Jančář L., Havel J.: *Computereinsatz in der Analytik, COMPANA '85, Jena 1985*; Abstr. No. 16.
34. Watkins S. L.: Commun. ACM *17*, 520 (1974).
35. Sillén L. G., Warnquist B.: Acta Chem. Scand. *22*, 3032 (1968); Arkiv Kemi *31*, 377 (1969).
36. Pavlíková N., Horák J., Havel J.: Scr. Fac. Sci. Nat. Univ. Purk. Brun. *11*, No. 9—10 (Chemia), 387 (1981).
37. Wallace R. M., Katz S. M.: J. Phys. Chem. *68*, 3890 (1964).
38. Varga L. P., Veatch J.: Anal. Chem. *39*, 1101 (1967).
39. Leggett D. J., McBryde W. A. A.: Anal. Chem. *47*, 1065 (1975).
40. Leggett D. J., Kelly S. L., Shine L. R., Wu Y. T., Chang D., Kadish K. M.: Talanta *30*, 579 (1983).
41. Kankare J. J.: Anal. Chem. *42*, 1322 (1970).
42. Fendler E., Fendler J.: *Advances in Physical Organic Chemistry*, Vol. 8, p. 271. Academic Press, London 1980.
43. Čermáková L., Rosendorfová J., Malát M.: Collect. Czech. Chem. Commun. *45*, 210 (1980).
44. Lasovský J., Grambal F., Rypka M.: Acta Univ. Palachi Olomouc., Fac. Rerum Nat. *61/62*, 51 (1979/1980).
45. Burešová I., Kubáň V., Sommer L.: Collect. Czech. Chem. Commun. *46*, 10č90 (1981).
46. Škarydová V., Čermáková L.: Collect. Czech. Chem. Commun. *47*, 776 (1982).
47. Hedbávný J.: *Thesis*. Purkyně University, Brno 1984.
48. Evtimova B. E.: Dokl. Bolg. Akad. Nauk *31*, 559 (1978).
49. Shtykov S. N., Sumina E. G., Chernova R. K., Semenenko E. V.: Zh. Anal. Khim. *39*, 1029 (1984).
50. Havel J., Jančářová I., Kubáň V.: Collect. Czech. Chem. Commun. *48*, 1290 (1983).
51. Poukl I. L., Shevchuk I. A.: Ukr. Khim. Zh. *44*, 275 (1978).

52. Psinko T. N., Pilipenko A. T., Volkova A. I.: Ukr. Khim. Zh. *49*, 476 (1983).
53. Massart D. L., Dijkstra A., Kaufman L.: *Evaluation and Optimization of Laboratory Methods and Analytical Procedures*, p. 213. Elsevier, Amsterdam 1978.
54. Deming S. N., Morgan S. L.: Anal. Chem. *45*, 278A (1973).

Translated by P. Adámek.